The Accuracy of 3D Parameters in Correspondence-based Techniques

M.A. Snyder

COINS Technical Report 86-28

July 1986

The Accuracy of 3D Parameters in Correspondence–based Techniques *

M. A. Snyder
Computer and Information Science
University of Massachusetts
Amherst, Mass. 01003

June 18, 1986

*A preliminary version of this work was presented at the Workshop on Motion, Charleston, S.C., May 1986. This research was supported by DARPA/Army ETL under grant DACA76-85-C-0008.

Abstract

In most treatments of motion analysis, image quantities such as the positions of interest points and FOEs, as well as environmental quantities such as depth and translation and rotation parameters, are treated as accurately known. Since the obtaining of such values is in essence an experimental measurement, and such measurements are by nature uncertain, such accuracy is almost never justifiable. In the absence of a quantitative analysis of the uncertainty in measured parameters, one is led to unjustifiably precise values for derived quantities.

In this paper we discuss the effect that uncertainties in the position of interest points in an image have on the determination of 3D parameters and on search regions for matches in successive frames. We will call this procedure *Uncertainty Analysis*. Our discussion is quite general, and can be applied to any correspondence–based technique for analyzing stereo or motion. As an example we quantitatively examine FOE–based algorithms for finding depth from motion for pure translation of the camera. We analyze two situations. First, we discuss the case where depths are initially unknown but can be found by measurement of image quantities (the "startup" process). We find the quantitative effect of uncertainty in these image quantities upon computed depth values. Second, we discuss the case of uncertainly known initial depth, and how this uncertainty affects the search area for the position of an interest point in future frames (the "updating" process). The latter analysis is relevant to any situation where initial estimates of depth are available, either from external processes such as laser ranging, or from an initial set of frames of a multi–frame analysis.

The primary conclusions of this paper are: 1) the uncertainty in the FOE has little effect on the calculation of search regions or the accuracy with which depths can be determined unless the uncertainty in the FOE is large compared to that of the image points, or if the inter–frame camera translation is a significant fraction of the depth; 2) when the inter–frame camera translation is a small fraction of the depth, the effect of uncertainty in the FOE on search regions or on depth calculations is small compared to that of the uncertainty in image points; 3) when the inter–frame camera translation is a small fraction of the depth, the uncertainty in the depth can have a significant effect on search regions, especially for image points far from the FOE.

We also use this uncertainty analysis to give a quantitative meaning and justification to two well known results in the analysis of motion: depth measurements are unreliable if (1) the interest point is close to the FOE or (2) the environmental point is far away from the camera.

1 Introduction

In theoretical treatments of image analysis, it is generally assumed that image points correspond directly to points in the (3D) environment through, for instance, central projection (a projective (Möbius) transformation). On a practical level, this is of course not the case. The most obvious reason why this is so is that any image resulting from a real sensor is spatially digitized (there is also a digitization in intensity, but we do not discuss that here). Suppose, for example, that we imagine an ideal sensor producing an ideal image, where points in the image correspond to points in the environment according to the equations of perspective projection. We will call this continuous image the *geometrical image* G of the environment. In the production of a discrete digital $N \times N$ image from G, information about the position of a point in G is lost, so that all that is known is the pixel in which the point lies. Thus, the position p of a point in G is known only to lie within an "uncertainty region" $\mathcal{R}$, which in this case is the pixel which contains p. If the image is given a Cartesian x–y coördinate system, the x– and y–coördinates of p are uncertain by an amount $\Delta x = \Delta y = 1/2$, where our units are such that a pixel is a 1×1 rectangle with sides parallel to the coördinate axes. We will call this *quantization uncertainty*.

In general, the position of the point may be more uncertain than that given by quantization uncertainty alone. A point in the environment may appear in the wrong place or with incorrect intensity as a result of sensor distortion and additive noise or aliasing. We will not treat these problems directly, but only their effects on the accuracy with which the position of image points can be determined.

Most stereo and motion techniques find the positions of corresponding points in two views either by using an interest operator (such as Moravec's [Mora1980] or Kitchen and Rosenfeld's [Kitc1982]) to select distinguished image points which are most easy to match, or by using a correlation measure, so we should consider how accurately the position of such image points can be determined. We confine our present discussion to interest points selected by some interest operator. Similar considerations hold for techniques which use a correlation measure.

Techniques which select interest points consist in optimizing some numerical measure. The location of the interest point is then defined as the center of the pixel in which the position of the optimum lies. If the interest measure is represented as a surface, with a peak corresponding to the optimum, then the uncertainty in the position of the interest point is related to the broadness of this peak; a broad peak corresponds to a larger uncertainty region than does a narrow peak. Since there is no canonical definition for "broadness," there can be no precise definition for the uncertainty region; hence, any conclusions based upon the size of the uncertainty region must be considered as only approximate.

We regard the production of the image of some scene as an experiment, since it corresponds to a measurement of the intensity distribution in the scene, projected onto the image plane. Consequently, the position of the optimum of the interest measure for a particular interest point is just the experimental value for the position p of the interest point F. We will call this the *nominal* position $\langle p \rangle$ of F. Note that the description of the nominal position makes absolutely no reference to the *structure* of the interest measure around its optimum. Consequently, the adjective "nominal" means "if uncertainty is neglected."

The question of how to choose the uncertainty region around the nominal position of F cannot, as noted, be given an unambiguous answer. One could, for instance, define the uncertainty region to consist of all pixels in a neighborhood of the nominal position $\langle p \rangle$ for which the interest measure has a value greater than (for instance) 80 % of its optimum value. But the choice of 80 % is surely an arbitrary one, reflecting the arbitrariness in the definition of the uncertainty region, and we do not intend to address that problem here.

The definition of the uncertainty region for an interest point F is an essentially mathematical one, but should have some physical interpretation. We propose that the uncertainty region should be chosen so that it is "highly likely" that the interest point in fact lies somewhere inside the uncertainty region. This means that we make the following physical interpretation of the uncertainty region: *any point in the uncertainty region for the interest point F is a possible position of the interest point.* This means that although in a particular experiment (i.e., a particular image) we find a definite position for the interest point (namely, its nominal position), any other point in the uncertainty region *could* have been found as the position of the interest point.

1.1 The uncertainty in environmental parameters

Let an interest point F have nominal position $\langle p \rangle$ and uncertainty region $\mathcal{R}$. As we noted in the previous section, the actual position p of F can be anywhere inside $\mathcal{R}$. Consider the environmental (i.e., $3D$) point P which gives rise to p in the image by, for example, perspective projection π:

$$\pi : P \rightarrow p.$$

Since p could in fact lie anywhere inside $\mathcal{R}$, it follows that there must be some region $\mathcal{R}^*$ in the environment which is mapped onto $\mathcal{R}$ by π:

$$\pi : \mathcal{R}^* \rightarrow \mathcal{R}.$$

Clearly, $P \in \mathcal{R}^*$. Thus, the uncertainty region $\mathcal{R}$ for p in the image gives rise to an uncertainty region $\mathcal{R}^*$ for P in the environment. This means that the location of P will also be uncertain.

Since many different environments can give rise to the same image,[1] the calculation of any environmental parameter must involve a comparison of at least two views of the environment. For the case of motion an environmental parameter such as depth is determined absolutely only if the inter–frame camera translation is known. If this camera parameter is not known, then only the depth relative to the camera translation can be found.

One way to make this comparison of the two views is to use correspondence–based techniques, most of which make use of some numerical measure to select points in both views, and then use a matching technique to determine the correspondence between the selected points. An environmental parameter is then determined from the relative position in the two images of the corresponding points. If the positions of the point in the two views are denoted by p_1 and p_2, and if the environmental parameter is the depth Z of the 3D point to which p_1 corresponds, then there is a functional relation between these three quantities. That is, any two determine the third. We write this functional relationship as

$$f(p_1, p_2, Z) = 0. \tag{1}$$

If uncertainties in the positions of the point in the two views are neglected, then the positions will be denoted by $\langle p_1 \rangle$ and $\langle p_2 \rangle$, and the depth will be given implicitly by

$$f(\langle p_1 \rangle, \langle p_2 \rangle, \langle Z \rangle) = 0. \tag{2}$$

However, as we have argued, image points can only be determined to lie inside some

[1]For instance, the camera could be imaging the 2D image from another camera.

uncertainty region. If we allow each of the points p_1 and p_2 to range independently over their respective uncertainty regions $\mathcal{R}_1$ and $\mathcal{R}_2$, it follows from (1) that Z must range over some uncertainty region as well. Since Z is just a number, this region is just an interval $\mathcal{I}$. We conclude that there must be a functional relationship between these three uncertainty regions which we write symbolically as

$$\mathcal{F}(\mathcal{R}_1, \mathcal{R}_2, \mathcal{I}) = 0. \tag{3}$$

What we mean by this equation is that if the uncertainty regions for two of the arguments of (1) are known, then the uncertainty region for the remaining argument can be calculated. This is done by allowing the former arguments to range over their respective uncertainty regions independently and using (1) to find the range of the latter argument.

There are three ways to choose these independent and dependent arguments. In the first way, we can consider p_1 and p_2 to be uncertainly known and calculate the range of values Z takes. This is the "startup" process, in which depth is initially unknown. Since Z is a number, the uncertainty region for Z is an interval $\left[Z^{\min},\ Z^{\max}\right]$. If all we know is that Z is somewhere inside this interval, then (assuming all values in the interval are equally probable) it is sensible to take the "best estimate" Z^{mean} for Z to be just the midpoint of the interval. We thus write the uncertainty interval as $[Z^{\text{mean}} - \delta Z,\ Z^{\text{mean}} + \delta Z]$, where δZ will be called the *uncertainty* in the depth. We also express this interval in the standard notation $Z = Z^{\text{mean}} \pm \delta Z$. Thus, all of the following mean the same thing:

$$\begin{aligned} Z &\in \left[Z^{\min},\ Z^{\max}\right] \\ Z &\in [Z^{\text{mean}} - \delta Z,\ Z^{\text{mean}} + \delta Z] \\ Z &= Z^{\text{mean}} \pm \delta Z. \end{aligned}$$

It should be noted that the "best" value Z^{mean} for the depth Z is not necessarily equal to the "nominal" value $\langle Z \rangle$ for Z. The reason for this is that $\langle Z \rangle$ is determined from equation (2), whereas Z^{mean} is determined as the midpoint of the uncertainty interval I, which is determined from "equation" (3). Since the two calculations are quite different, there is no reason to expect the equality of the two values for Z. Indeed, in Section 4 we will see examples where $\langle Z \rangle$ and Z^{mean} are unequal.

The second way of viewing (3) is to take p_1 and Z as independent arguments in (1), and calculate the uncertainty region for p_2. This region is just the search region for p_2, since the uncertainty region is exactly the possible positions of p_2 consistent (via (1)) with the uncertainties in p_1 and Z. This way of looking at (3) thus corresponds to the search portion of the updating process.

The third way is identical to the second, but with the roles of p_1 and p_2 reversed. That is, the uncertainty in the values of p_2 and Z are used to *calculate* the uncertainty region $\mathcal{R}_1^{\text{calc}}$ for p_1. Since this requires the uncertainty in Z to be determined independently from that in the position of p_1, and since the uncertainty region $\mathcal{R}_1$ for p_1 can be calculated *directly from the image* in this frame, we can compare $\mathcal{R}_1^{\text{calc}}$ and $\mathcal{R}_1$. Such a comparison can lead to the testing of initial depth estimates derived from, for example, laser ranging, and could lead to a refinement of depth estimates.

In this work, we will consider only the first two ways of looking at (3). What we have referred to as startup and updating have also been referred to as *bootstrapping* and *refinement* [Waxm1985a].

The assumption that all values of Z within an interval are equally likely, and that the interest point is equally likely to be found anywhere inside of, and no probability of being found outside of, its uncertainty region is a strong one. A more careful and precise approach to the problem would be to associate a probability distribution for two of the three quantities, and then use the functional relationship (1) to find the probability distribution for the third quantity. However, what is important in practice is to constrain the search region. An exact probability of match location is not so useful. In this paper we do not consider such probabilistic approaches, leaving their analysis for future work

Determination of the functional relationship (3) depends on the specific situation under investigation. In this paper, we examine the case of a camera having purely translational motion at constant velocity through a rigid environment, and consider FOE–based methods for finding environmental depth (a depth map) by matching points between two or more frames from a dynamic image sequence. We consider this situation both because it can, with a few simplifying assumptions about the shape of the uncertainty regions, be solved mainly analytically, and because it corresponds to motion that is of practical interest, for instance in autonomous navigation [Waxm1985b]).

In Section 2 we derive the basic equations for FOE–based motion in a form which will be useful for our analysis. In Section 3 we make some definitions which will simplify our discussion. The main results of the paper are derived in Section 4. In section 5 we give numerical examples of the application of these ideas to several situations of practical interest. In Section 6 we summarize our results. The reader who is uninterested in the calculational details can consult this section and Section 5 for the main results of the work. There are four appendices. In Appendix A we derive a result used in Section 4 to calculate search regions. In Appendix B we give a quantitative justification for two well known qualitative results in motion analysis. In Appendix C we give the details of how

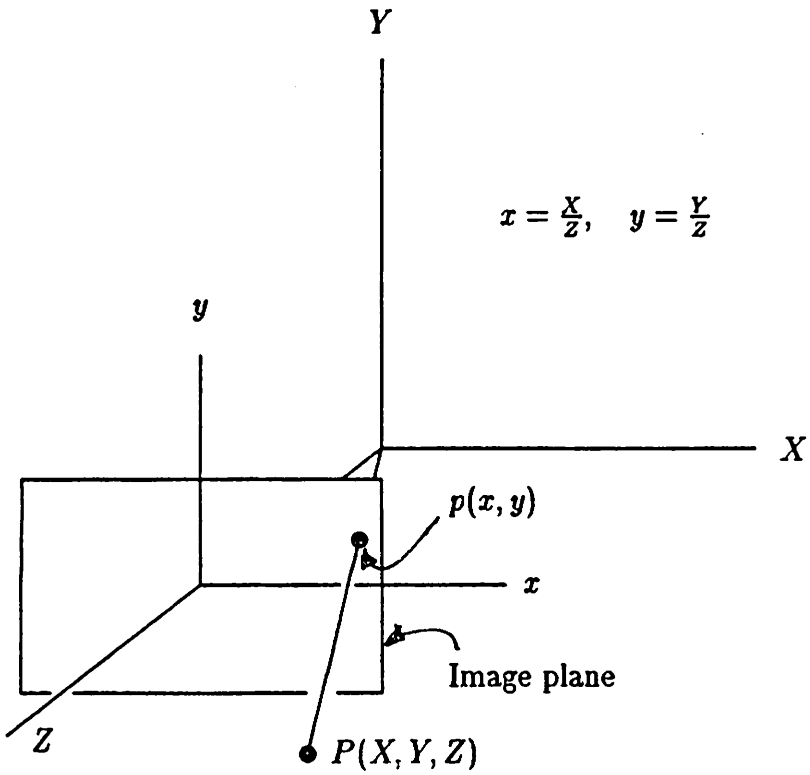

Figure 1: Perspective projection

one calculates depth uncertainties from uncertain feature positions. In Appendix D we summarize the numerical results for search regions.

2 Basic Equations

We assume the usual geometry of perspective projection, as illustrated in Figure 1, where we have chosen the focal length of the projection to be unity. The camera coordinate system is denoted by (X, Y, Z). As mentioned in the introduction, the camera is moving with constant speed in the $+Z$ direction through a rigid environment; this is equivalent to a rigid environment moving at the same constant speed in the $-Z$ direction toward a fixed motionless camera.

In the case of uniform translation of the camera toward a rigid environment, the motion of the image point p of some 3D point P is analytically simple [Long1980]; each point p moves along a straight trajectory, and and all such straight lines intersect at a single point Q. Since all image points move away from Q, this point is called the *Focus of Expansion* (*FOE*).

If we let $D(t)$ be the distance of p from the FOE at time t, and let $Z(t)$ be the Z−coördinate of the 3D point P to which p corresponds, then it is easy to show [Long1980] that

$$\frac{D(t') - D(t)}{D(t)} = \frac{Z(t) - Z(t')}{Z(t')}, \tag{4}$$

where t and t' are any two times. We shall refer to $Z(t)$ as the *depth* of P at time t. It follows immediately from (4) that the quantity $D(t)Z(t)$ is a *constant of the motion*, i.e.,

$$D(t)Z(t) = D(t')Z(t') \tag{5}$$

for all t and t'.

We assume that the environment is sampled at regular intervals t_n, where $t_n = n\tau$ ($n = 0, 1, \ldots, N$), and τ is the (constant) interval between successive frames. Since the motion of the camera is uniform, we let T be the distance the camera moves toward the environment in the time interval τ. We take $t' = t_{n+1}$, $t = t_n$ in (4), and define:

$$D_n = D(t_n); \quad Z_n = Z(t_n); \quad \Delta D_n = D_{n+1} - D_n$$

(see Figure 2). Then since $T = Z_n - Z_{n+1}$ for all n,

$$\frac{\Delta D_n}{D_n} = \frac{D_{n+1} - D_n}{D_n} = \frac{Z_n - Z_{n+1}}{Z_{n+1}} = \frac{T}{Z_{n+1}}. \tag{6}$$

We can then rewrite (6) as

$$D_{n+1} = K_n D_n, \tag{7}$$

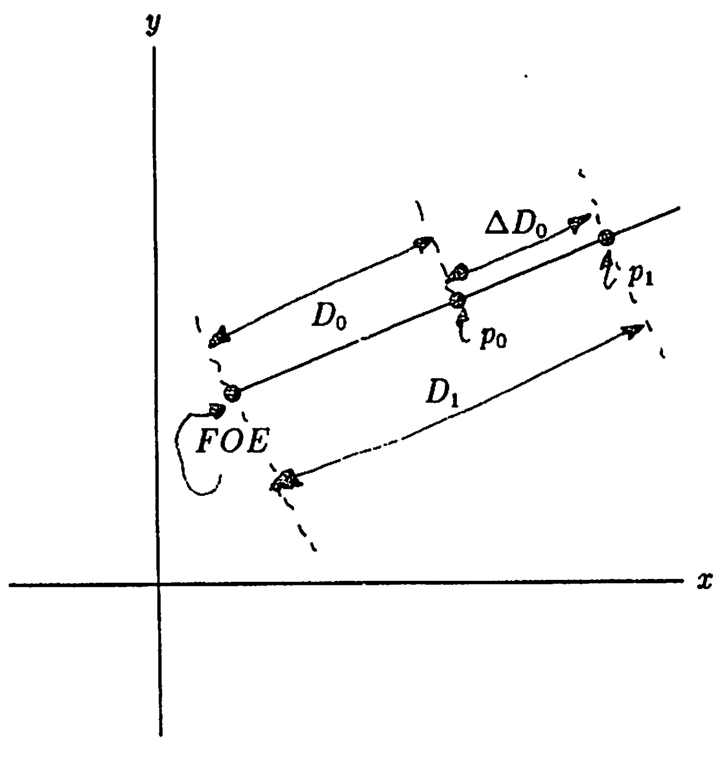

Figure 2: The displacement path

where

$$K_n = 1 + \frac{T}{Z_{n+1}} = \frac{Z_n}{Z_{n+1}} = \frac{Z_n}{Z_n - T} > K_{n-1} > 1. \tag{8}$$

Equation (7) will play a central role in our analysis.

If we denote by p_n the position of the projected environmental point P at time t_n, then all the p_n (for $n = 0, \ldots, N$) lie along a line. Clearly, the displacements of p between frames are constrained to lie along this line, so we will call this line the *displacement path* (see Figure 2).

If we denote by $\vec{r}_j$ the vector from the FOE to p_j, $j = 0, \ldots, N$, then since all the p_j lie along the displacement path equation (7) implies that

$$\vec{r}_{n+1} = K_n \vec{r}_n. \tag{9}$$

Note that $|\vec{r}_j| = D_j$. Equation (9) will prove to be very useful in the next sections.

3 Definitions

Let F be an interest point in the image. We denote by F_n the instance of F in frame n at time t_n. The position of F_n will be the point $p_n = (x_n, y_n)$. The nominal value that any quantity Q takes will be denoted by enclosing Q in angle brackets: $\langle Q \rangle$. Thus, the nominal position of F_n will be denoted by $\langle p_n \rangle = (\langle x_n \rangle, \langle y_n \rangle)$. Recall that the nominal value $\langle Q \rangle$ is the value that Q would have in the absence of uncertainty. We will refer to the line that passes through the nominal positions of the FOE, F_0, F_1, ..., F_n as the *nominal displacement path (NDP)*. We will use the adjective *environmental* to be synonymous with *3D*.

As noted in the introduction, the position of F_n is uncertain but can be assumed to be in an uncertainty region $\mathcal{R}_n$ which contains the nominal point $\langle p \rangle_n$. In order to investigate the situation analytically, we must make some assumption about $\mathcal{R}_n$. We will choose $\mathcal{R}_n$ to be a rectangle R_n centered at $\langle p_n \rangle$, with sides parallel to the $x-$ and $y-$axes of length $2\Delta x_n$ and $2\Delta y_n$, respectively. We will denote these sides as $\{2\Delta x_n, 2\Delta y_n\}$. Thus,

$$(x_n, y_n) = p_n \in R_n \iff \begin{cases} \langle x_n \rangle - \Delta x_n \leq x_n \leq \langle x_n \rangle + \Delta x_n, \\ \langle y_n \rangle - \Delta y_n \leq y_n \leq \langle y_n \rangle + \Delta y_n \end{cases} . \tag{10}$$

We assume, similarly, that the location of the FOE is uncertain, but lies within a rectangle R of sides $\{2\Delta x, 2\Delta y\}$ centered at the nominal position $\langle \text{FOE} \rangle$ of the FOE. We choose the coördinate system such that $\langle \text{FOE} \rangle$ is at the origin $(0,0)$ of the coördinate system.

3.1 Comments

We note that the uncertainties in the position of features are due only to the structure of the image. The uncertainty in the position of the FOE, however, arises from two sources. The first is the technique used to identify the position of the FOE. The second is the uncertainty in the direction of translation of the camera. We have assumed that the camera is translating along the Z-axis, but for mechanical reasons this may be difficult to enforce. If we let the uncertainty in the translation vector be $\delta\vec{T}$ and let T be the z-component of $\vec{T}$, then it can be easily shown that the uncertainty region for the FOE due to this uncertainty alone is a rectangle centered at $(0,0)$, with sides

$$\{2\Delta x,\ 2\Delta y\} = \frac{N}{\tan[\gamma/2]} \left\{ \frac{\delta T_x}{T},\ \frac{\delta T_y}{T} \right\}, \tag{11}$$

where γ is the field of view of the camera, and the image has a resolution of $N \times N$ pixels. It should be noted that for typical values of N and γ, even a small uncertainty in the direction of translation can give a large uncertainty rectangle for the FOE. For instance, for $N = 256$ and $\gamma = 30°$, a $1°$ uncertainty in the direction of $\vec{T}$ will give an 8×8 uncertainty rectangle for the FOE. Clearly, it is in general important for the direction of translation of the camera to be accurately known (see, however, the comments at the end of Section 4.1.1).

The assumption that $\langle p_n \rangle$ is at the center of R_n is equivalent to equating the "best" and "nominal" positions of F_n. This, and the assumption that the uncertainty regions are rectangular, is made for simplicity of exposition only; other choices could be made, but would require a more complicated analysis. The results of this paper could be applied to a technique which uses non-rectangular uncertainty regions by, for instance, approximating the given uncertainty region by the smallest rectangle with sides parallel to the coördinate axes which contains the given uncertainty region. In that event, the results of this paper would give conservative estimates for uncertainties.

4 Startup and Updating

In this section we analyze the effect of uncertainties on the computation of depth values from the position of an interest point in two frames of a dynamic image sequence (the "startup" process), and on the search region for the interest point in subsequent frames (the search portion of the "updating" process).

In order to analyze the startup and updating processes efficiently, we will find it useful to derive some preliminary results. We first assume that the uncertainty regions for the

FOE and for the interest point in one frame of the dynamic image sequence are known. For simplicity of exposition, we will call this frame the "0" frame. We assume that the depth Z_0 of the environmental point in the chosen frame is known, in one case accurately, and in the other, uncertainly, and in each case calculate the search region for the interest point in the next frame, the "1" frame. This is done in Section 4.1. Although these results are used in the present work as a basis for analyzing the startup and updating processes, they would of course be relevant to any situation in which initial depth estimates were available by independent means.

In the final two sections, we use the preliminary results of section 4.1 to discuss the startup and updating processes. In Section 4.2 we discuss the calculation of the depth Z_1 from uncertainly known *FOE*, F_0, and F_1 (startup), and in section 4.3 we use this result to find the search region for the interest point in the *third* frame, F_2 (updating).

4.1 Preliminary analysis: Calculating the search region $\mathcal{R}_1$ for F_1 from uncertainly known FOE and F_0

4.1.1 Accurately known depth Z_0 and inter–frame camera translation T

We assume the position of the FOE and of F_0 to be uncertain (see Figure 3), but that K_0 (i.e., Z_0 and T) is accurately known, i.e., there is no uncertainty associated with K_0.

Let the vector from $\langle\text{FOE}\rangle$ to $\langle p_0\rangle$ be denoted by $\langle\vec{r}_0\rangle$, and that from $\langle\text{FOE}\rangle$ to $\langle p_1\rangle$ by $\langle\vec{r}_1\rangle$ (see Figure 4). If uncertainties are neglected, then we have from (9) that:

$$\langle\vec{r}_1\rangle = K_0\langle\vec{r}_0\rangle. \tag{12}$$

This would then determine $\langle p_1\rangle$. However, both the position of the FOE and the position

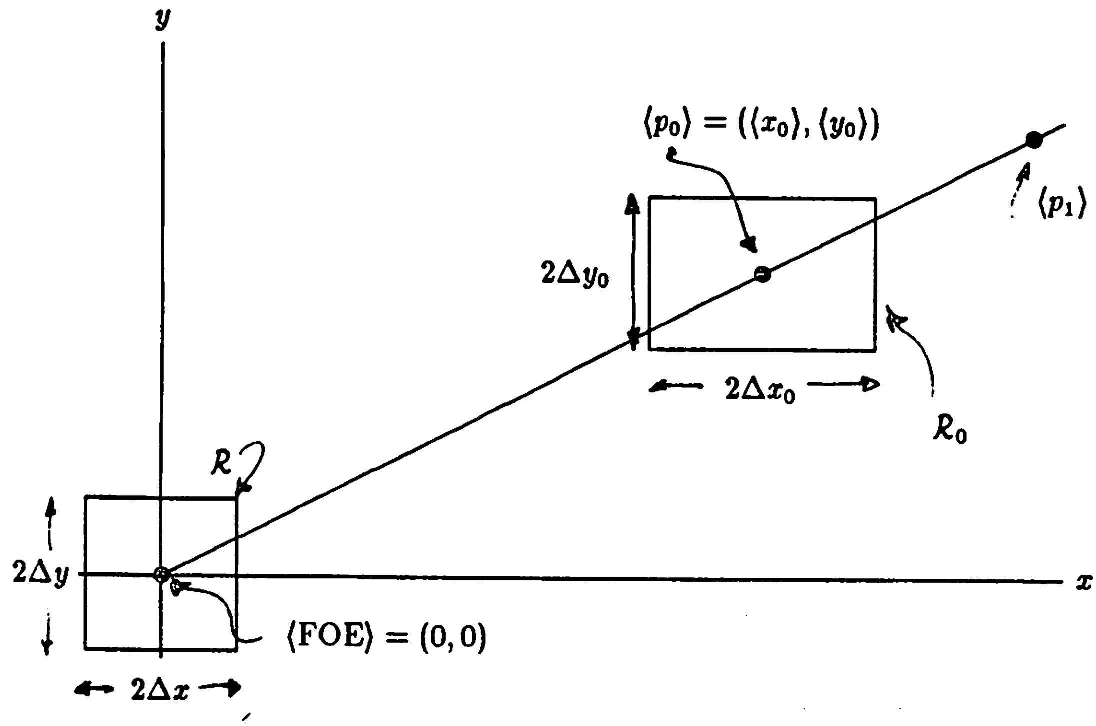

Figure 3: Uncertainty Regions

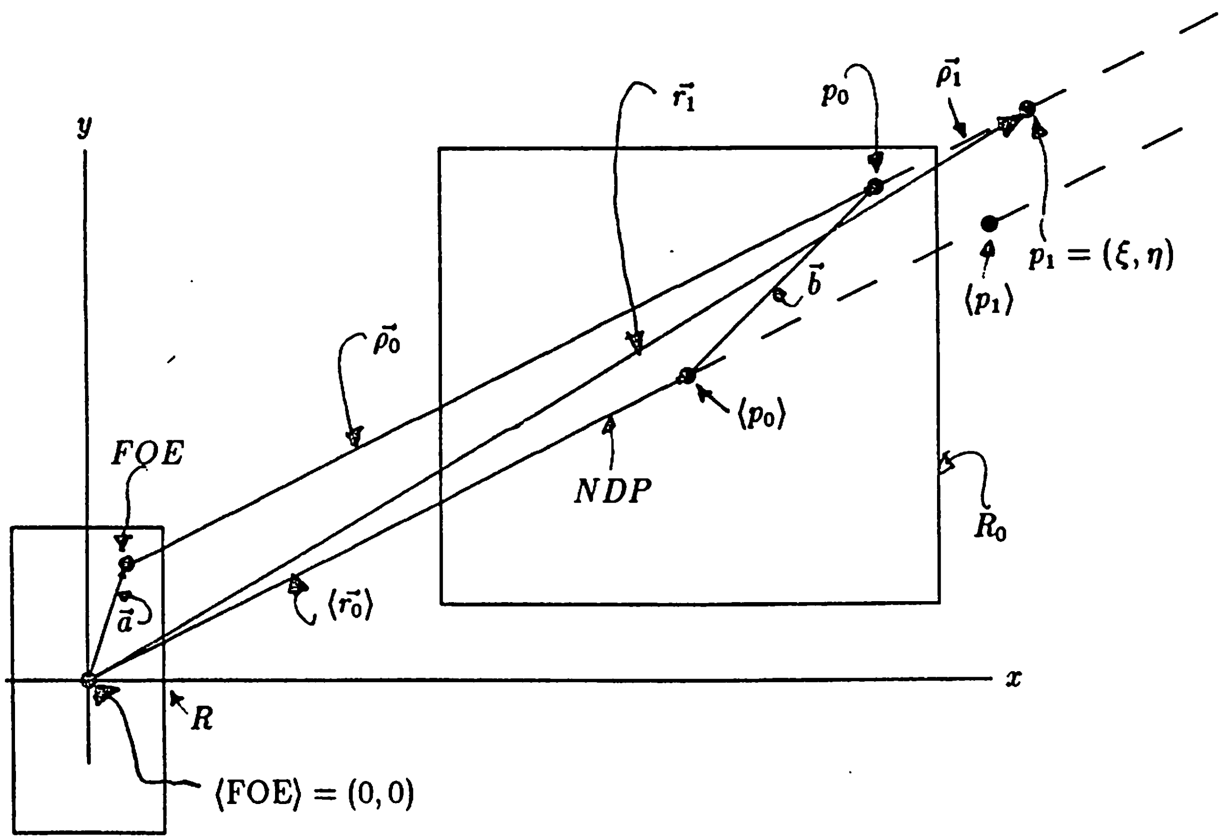

Figure 4: Geometry for finding $\mathcal{R}_1$. Note that $\vec{\rho_1}$ is the vector from FOE to p_1.

p_0 of F_0 are assumed uncertain; we know only that each point is somewhere inside its respective uncertainty rectangle:

$$p_0 \in R_0, \quad FOE \in R. \tag{13}$$

This is illustrated in Figure 4, where we have indicated possible choices for FOE and p_0. If $\vec{\rho_0}$ denotes the vector from FOE to p_0, and $\vec{\rho_1}$ denotes the vector from FOE to p_1, then from (9):

$$\vec{\rho_1} = K_0 \vec{\rho_0}. \tag{14}$$

The problem is to find the region $\mathcal{R}_1$ over which the tip of $\vec{\rho_1}$ ranges as the FOE ranges over R and p_0 ranges over R_0. This must then be the area in the second frame which must be searched for F_1. This region can be found as follows. Let $\vec{a}$ be the vector from ⟨FOE⟩ to FOE, $\vec{b}$ be the vector from $\langle p_0 \rangle$ to p_0, and $\vec{r_1}$ be the vector from ⟨FOE⟩ to p_1. The search region $\mathcal{R}_1$ thus corresponds to the possible positions of the tip of $\vec{r_1}$, subject to the constraint (13). If we write

$$\begin{aligned}
\langle \vec{r_0} \rangle &= \langle x_0 \rangle \hat{x} + \langle y_0 \rangle \hat{y}, \\
\vec{a} &= a_1 \hat{x} + a_2 \hat{y}, \\
\vec{b} &= b_1 \hat{x} + b_2 \hat{y}, \\
\vec{r_1} &= \xi \hat{x} + \eta \hat{y},
\end{aligned}$$

where $\hat{x}$ and $\hat{y}$ are unit vectors along the coordinate axes, then from Figure 4,

$$\begin{aligned}
\vec{\rho_0} &= \langle \vec{r_0} \rangle + \vec{b} - \vec{a}, \\
\vec{r_1} &= \vec{\rho_1} + \vec{a}.
\end{aligned}$$

Hence, from (14),

$$\vec{r}_1 = K_0\langle\vec{r}_0\rangle + K_0\vec{b} - (K_0 - 1)\,\vec{a}. \tag{15}$$

Taking the components of this, we find:

$$\xi = K_0\langle x_0\rangle + K_0 b_1 - (K_0 - 1)\,a_1, \tag{16}$$

$$\eta = K_0\langle y_0\rangle + K_0 b_2 - (K_0 - 1)\,a_2. \tag{17}$$

The region $\mathcal{R}_1$ is then found by determining the range of values ξ and η take as $\vec{a}$ and $\vec{b}$ range over the uncertainty regions R and R_0.

This is equivalent to the following mathematical problem: Find the maximum and minimum values that ξ and η take subject to the conditions on a_1, a_2, b_1, and b_2:

$$\begin{aligned} -\Delta x &\leq a_1 \leq +\Delta x, \\ -\Delta x_0 &\leq b_1 \leq +\Delta x_0, \\ -\Delta y &\leq a_2 \leq +\Delta y, \\ -\Delta y_0 &\leq b_2 \leq +\Delta y_0. \end{aligned} \tag{18}$$

Since the limits on a_2 are independent of a_1 (and vice–versa), the range of values that a_2 can take is independent of the value of a_1 (and vice–versa). An identical statement holds for b_1 and b_2. Consequently, equations (16) and (17) are decoupled, and can be treated separately. Note that this result is critically dependent on the fact that both uncertainty regions are rectangles.[2] If this is not the case, then equations (16) and (17) are coupled, and cannot be treated independently.

[2] For instance, if R were a circle of radius λ, then $a_2 = \sqrt{\lambda^2 - a_1^2}$, so a_2 would not be independent of a_1, nor would its limits.

Since the equations for ξ and η are indeed decoupled, we immediately conclude that the search region $\mathcal{R}_1$ is a rectangle R_1 with sides parallel to the coordinate axes. It remains only to find the sides and the center of the rectangle. Since equations (16) and (17) are identical except for the names of the quantities involved, we need consider only one of them, for instance (16). The result which follows from (17) is then trivially obtained by substituting y–components for x–components.

We want to find the maximum/minimum values of ξ as FOE and p_0 range (independently) over their respective uncertainty regions. That is, we want to find the maximum/minimum values for ξ if a_1 and b_1 are subject to (18). Since $K_0 > 1$, this problem is trivial: ξ is a maximum/minimum when b_1 is a maximum/minimum and a_1 is a minimum/maximum. Thus

$$\begin{aligned}\xi_{\min}^{\max} &= K_0\langle x_0\rangle + K_0(\pm\Delta x_0) - (K_0 - 1)(\mp\Delta x) \\ &= K_0\langle x_0\rangle \pm \Big(K_0\Delta x_0 + (K_0 - 1)\Delta x\Big). \end{aligned} \tag{19}$$

If we write this as $\xi_{\min}^{\max} = \xi^{\text{mean}} \pm \Delta\xi$, then

$$\begin{aligned}\xi^{\text{mean}} &= K_0\langle x_0\rangle, \\ \Delta\xi &= K_0\Delta x_0 + (K_0 - 1)\Delta x.\end{aligned}$$

We can then immediately write down the solution for $\eta_{\min}^{\max}$ by substituting y everywhere we see x above: $\eta_{\min}^{\max} = \eta^{\text{mean}} \pm \Delta\eta$, where

$$\begin{aligned}\eta^{\text{mean}} &= K_0\langle y_0\rangle, \\ \Delta\eta &= K_0\Delta y_0 + (K_0 - 1)\Delta y.\end{aligned}$$

Therefore $\mathcal{R}_1$ is a rectangle R_1 centered at

$$(K_0\langle x_0\rangle,\ K_0\langle y_0\rangle) = K_0\left(\langle x_0\rangle,\ \langle y_0\rangle\right), \tag{20}$$

and of sides

$$\{2\left[K_0\Delta x_0 + (K_0 - 1)\Delta x\right],\ 2\left[K_0\Delta y_0 + (K_0 - 1)\Delta y\right]\}. \tag{21}$$

We draw several conclusions from this preliminary analysis. Under the stated conditions of uncertainly known FOE and p_0, and accurately known Z_0 and T:

- The center of the search rectangle is identical to the nominal position $\langle p_1\rangle$ of F_1. Thus, in this case, the "best" and "nominal" values coincide.

- If the camera displacement is small compared to the depth, $T \ll Z_0$, then according to (8), $K_0 - 1 \ll 1$. Therefore the sides of the search rectangle R_1 are only weakly dependent on Δx and Δy. This means that *the uncertainty in the position of the FOE has in this case very little effect on the search region*: it is the uncertainty in the location of F_0 which is most significant. In such cases the size of the search rectangle is about the same as that of the uncertainty rectangle R_0.

One should note, however, that this does *not* mean that the uncertainty in the direction of translation has little effect on the search region, since (as was discussed in Section 3) even a small uncertainty in the direction of translation can give a large uncertainty in the FOE.

Although all the results we derive hold for arbitrary values of T and Z, we will often consider the case where $T \ll Z$. The reason for this is that many of our results take a particularly simple form when this limiting case is considered, and hence general statements about the effect of particular kinds of uncertainties can be made. When T is *not* small compared to Z, then the only comment one can generally make is that everything is important, i.e., the "exact" formulas must be used.

4.1.2 Uncertainly known depth Z_0 and inter–frame camera translation T

In this case we consider the same situation as in Section 4.1.1 except that we drop the assumption that Z_0 and T, and hence K_0, are accurately known. Thus we assume that Z_0 is known only to be within δZ_0 of Z_0^{mean}. Since here Z_0 is assumed to be a directly measured quantity, we identify Z_0^{mean} and $\langle Z_0 \rangle$. Thus,

$$Z_0 = \langle Z_0 \rangle \pm \delta Z_0.$$

From (8) it follows that K_0 is uncertain, but must lie in the interval I:

$$K_0 \in I = [K_0^{\text{mean}} - \delta K_0,\ K_0^{\text{mean}} + \delta K_0],$$

where K_0^{mean} is the best estimate for K_0, and δK_0 is the uncertainty in K_0. We can easily calculate K_0^{mean} and δK_0 from $\langle Z_0 \rangle$ and δZ_0. We have, from (8), that

$$K_0 = \frac{Z_0}{Z_0 - T}. \tag{22}$$

We assume that T is uncertainly known and given by $T = \langle T \rangle \pm \delta T$.

Since K_0 is a monotonically decreasing function of Z_0, but a monotonically increasing function of T, we have that

$$K_0^{\text{mean}} \pm \delta K_0 = \frac{\langle Z_0 \rangle \mp \delta Z_0}{\langle Z_0 \rangle \mp \delta Z_0 - (\langle T \rangle \pm \delta T)}.$$

We then easily find that to first order in the uncertainties δZ_0 and δT

$$K_0^{\mathrm{mean}} = \frac{\langle Z_0 \rangle}{\langle Z_0 \rangle - \langle T \rangle}, \tag{23}$$

$$\delta K_0 = K_0^{\mathrm{mean}}(K_0^{\mathrm{mean}} - 1)\frac{\delta Z_0}{\langle Z_0 \rangle} + [K_0^{\mathrm{mean}}]^2 \frac{\delta T}{\langle Z_0 \rangle}. \tag{24}$$

Since K_0^{mean} is identical to the value $\langle K \rangle_0$ that would be obtained by plugging the nominal values of Z_0 and T into (8), we drop the distinction between K_0^{mean} and $\langle K_0 \rangle$.

We then have from (23) that

$$\langle K_0 \rangle - 1 = \frac{\langle T \rangle}{\langle Z_0 \rangle - \langle T \rangle} = \langle K_0 \rangle \frac{\langle T \rangle}{\langle Z_0 \rangle}. \tag{25}$$

Using (25), we can then write $K_0 = \langle K_0 \rangle \pm \delta K_0$, where

$$\langle K_0 \rangle = \frac{\langle Z_0 \rangle}{\langle Z_0 \rangle - \langle T \rangle}, \tag{26}$$

$$\delta K_0 = \langle K_0 \rangle (\langle K_0 \rangle - 1)\, [\epsilon] \tag{27}$$

and

$$\epsilon = \frac{\delta Z_0}{\langle Z_0 \rangle} + \frac{\delta T}{\langle T \rangle}. \tag{28}$$

The quantity ϵ is the sum of the *relative uncertainty* $\delta Z_0 / \langle Z_0 \rangle$ in the depth, and that in the inter-frame camera translation.

Recall that we have assumed a uniform distribution of the possible values for Z_0 in its uncertainty interval. Strictly speaking, this will *not* give a uniform distribution for the values of K_0 in *its* uncertainty interval. However, we must ignore such subtleties here, since we are not taking into account any non-uniform probability distributions.

In Section 4.1.1, we found that for accurate K_0 the search region for the position p_1 of F_1 was the rectangle R_1 described by equations (20) and (21). Since the properties of this rectangle depend on the value of K_0, we shall write it as $R_1(K_0)$. If we now allow K_0 to range over an interval I, the search region $\mathcal{R}_1$ for p_1 must be the union of all the $R_1(K_0)$, for K_0 in I:

$$\mathcal{R}_1 = \bigcup_{K_0 \in I} R_1(K_0).$$

In Appendix A we show that $\mathcal{R}_1$ is the intersection of a "wedge," described in the appendix, with a rectangle R_1^* which we will now calculate. The rectangle R_1^* can also serve as a simple approximation to $\mathcal{R}_1$ in many cases (see Section 5). The rectangle R_1^* is the smallest rectangle having sides parallel to the coördinate axes which contains the region $\mathcal{R}_1$. This can be found by a procedure similar to that used in Section 4.1.1. We use the same notation as before. The $x-$ and $y-$coördinates again decouple, so we need look only at the $x-$coördinate. From (19), the right-hand side (RHS) and left-hand side (LHS) of $R_1(K_0)$ are located at:

$$\begin{aligned} \text{RHS} &= \xi_{\max} = K_0\langle x_0\rangle + (K_0\Delta x_0 + (K_0 - 1)\Delta x), \\ \text{LHS} &= \xi_{\min} = K_0\langle x_0\rangle - (K_0\Delta x_0 + (K_0 - 1)\Delta x). \end{aligned}$$

The RHS is a monotonically increasing function of K_0. The LHS is a monotonically increasing or decreasing function of K_0 depending on whether $\langle x_0\rangle$ is greater or less, respectively, than $\Delta x + \Delta x_0$. We shall consider first the former case. This amounts to assuming that the projections of R and R_0 on the $x-$axis do not overlap.

The non–overlapping case

In the non–overlapping case, $\langle x_0 \rangle > \Delta x + \Delta x_0$. Since the RHS and LHS are then both monotonically increasing functions of K_0, the RHS (LHS) has its largest (smallest) value when K_0 is as large (small) as possible, i.e., when $K_0 = \langle K_0 \rangle + \delta K_0$ $(K_0 = \langle K_0 \rangle - \delta K_0)$. This means that the RHS/LHS of the search rectangle must lie at:

$$\xi = [\langle K_0 \rangle \pm \delta K_0]\langle x_0 \rangle \pm [(\langle K_0 \rangle \pm \delta K_0)\Delta x_0 + (\langle K_0 \rangle \pm \delta K_0 - 1)\Delta x],$$

where the upper sign is taken for the RHS, and the lower sign for the LHS, of the search rectangle. Thus, the RHS/LHS of $\mathcal{R}$ is at:

$$\xi = [\langle K_0 \rangle \langle x_0 \rangle + \delta K_0(\Delta x_0 + \Delta x)] \pm [\langle x_0 \rangle \delta K_0 + \langle K_0 \rangle \Delta x_0 + (\langle K_0 \rangle - 1)\Delta x].$$

An identical argument shows that the upper/lower side of $\mathcal{R}$ is (assuming that the projections of R and R_0 on the y–axis do not overlap) at

$$\eta = [\langle K_0 \rangle \langle y_0 \rangle + \delta K_0(\Delta y_0 + \Delta y)] \pm [\langle y_0 \rangle \delta K_0 + \langle K_0 \rangle \Delta y_0 + (\langle K_0 \rangle - 1)\Delta y].$$

Consequently, if R and R_0 do not overlap, the search region $\mathcal{R}$ is the intersection of a wedge with a rectangle R_1^* centered at

$$(\langle K_0 \rangle \langle x_0 \rangle + \delta K_0(\Delta x_0 + \Delta x), \langle K_0 \rangle \langle y_0 \rangle + \delta K_0(\Delta y_0 + \Delta y)), \tag{29}$$

having sides

$$\{2\left[\langle x_0 \rangle \delta K_0 + \langle K_0 \rangle \Delta x_0 + (\langle K_0 \rangle - 1)\Delta x\right], 2\left[\langle y_0 \rangle \delta K_0 + \langle K_0 \rangle \Delta y_0 + (\langle K_0 \rangle - 1)\Delta y\right]\}. \tag{30}$$

Note that the center of R_1^* is *not* at the nominal position $\langle p_1 \rangle$ of F_1, unlike in the previous case; indeed, the center of R_1^* is in general not even along the nominal displacement path (although the deviation from the NDP is usually small, since it is second order in the uncertainties).

The overlapping case

We now investigate the case where the projections of R and R_0 on the x– or y–axis overlap. Again, we need only consider the overlap on the x–axis. In the overlapping case, $\langle x_0 \rangle \leq \Delta x + \Delta x_0$. If this is true, then the LHS of $R_1(K_0)$ is a monotonically non-decreasing function of K_0. Hence, for $K_0 \in I$ the LHS has its smallest value when K_0 is as *large* as possible (cf. the previous case!), i.e., when $K_0 = \langle K_0 \rangle + \delta K_0$. This means that the RHS/LHS of R is at

$$\xi = [\langle K_0 \rangle + \delta K_0] \langle x_0 \rangle \pm ([\langle K_0 \rangle + \delta K_0] \Delta x_0 + [\langle K_0 \rangle + \delta K_0 - 1] \Delta x) . \tag{31}$$

It then follows *mutatis mutandem* that if the projections of R and R_0 onto the y–axis overlap, i.e., if $\langle y_0 \rangle \leq \Delta y + \Delta y_0$, then the upper/lower side of R_1^* is at

$$\eta = [\langle K_0 \rangle + \delta K_0] \langle y_0 \rangle \pm ([\langle K_0 \rangle + \delta K_0] \Delta y_0 + [\langle K_0 \rangle + \delta K_0 - 1] \Delta y) . \tag{32}$$

We may summarize these results as follows: Let ω be x or y. Then the rectangle R_1^* has center at

$$(C_x, C_y) \tag{33}$$

and has sides

$$(2S_x, 2S_y), \tag{34}$$

where

$$C_\omega = \left\{ \begin{array}{l} (\langle K_0\rangle + \delta K_0)\langle\omega_0\rangle \\ \\ \langle K_o\rangle\langle\omega_0\rangle + \delta K_0(\Delta\omega + \Delta\omega_0) \end{array} \right\}, \tag{35}$$

and

$$S_\omega = \left\{ \begin{array}{l} (\langle K_0\rangle + \delta K_0)\Delta\omega_0 + (\langle K_0\rangle + \delta K_0 - 1)\Delta\omega \\ \\ \langle\omega_0\rangle\delta K_0 + \langle K_0\rangle\Delta\omega_0 + (\langle K_0\rangle - 1)\Delta\omega \end{array} \right\}, \tag{36}$$

where the upper (lower) entry in curly brackets is chosen if the projection of the rectangles R and R_0 on the ω–axis do (do not) overlap. Substituting for δK_0 from (27) into these expressions, we find that

$$C_\omega = \left\{ \begin{array}{l} \langle K_0\rangle\langle\omega_0\rangle\left\{1 + (\langle K_0\rangle - 1)\,[\epsilon]\right\} \\ \\ \langle K_0\rangle\langle\omega_0\rangle\left\{1 + (\langle K_0\rangle - 1)\,[\epsilon]\left[\frac{\Delta\omega+\Delta\omega_0}{\langle\omega_0\rangle}\right]\right\} \end{array} \right\}, \tag{37}$$

where ϵ is defined by (28). Note that the coefficient common to both entries is just the ω–coördinate of the nominal position

$$\langle p_1\rangle = (\langle K_0\rangle\langle x_0\rangle, \langle K_0\rangle\langle y_0\rangle) = \langle K_0\rangle(\langle x_0\rangle, \langle y_0\rangle)$$

of the interest point in the next frame, frame 1. Similarly, the sides of R_1^* are given by

$$S_\omega = \left\{ \begin{array}{l} \langle K_0\rangle\Delta\omega_0 + (\langle K_0\rangle - 1)\Delta\omega + \langle K_0\rangle\,(\langle K_0\rangle - 1)\,[\epsilon]\,\{\Delta\omega + \Delta\omega_0\} \\ \\ \langle K_0\rangle\Delta\omega_0 + (\langle K_0\rangle - 1)\Delta\omega + \langle K_0\rangle\,(\langle K_0\rangle - 1)\,[\epsilon]\,\{\langle\omega_0\rangle\} \end{array} \right\}. \tag{38}$$

Please recall that the actual search region is the intersection of the rectangle R_1^* described above and the "wedge" described in Appendix A.

We now note the following from (33,34) with (37,38):

- When the inter-frame camera translation T is much smaller than the depth Z_0, i.e., $\langle K_0 \rangle - 1 \ll 1$, then just as in the case of accurately known Z_0 and T, the uncertainty in the position of the FOE has little effect on the search region. The reason for this is that $\Delta\omega$ (i.e., Δx or Δy) is multiplied by the small quantity $\langle K_0 \rangle - 1$ in expressions (37) and (38).

- When $\langle K_0 \rangle - 1 \ll 1$, the uncertainty in the depth and camera translation have little effect on the position of the center of R_1^*, since the quantity ϵ (which measures this uncertainty) always appears in (37) multiplied by $\langle K_0 \rangle - 1$, which is by assumption small. (Recall that the lower expression in (37) is to be used only when there is no overlap, i.e., when $[(\Delta\omega + \Delta\omega_0)/\langle\omega_0\rangle] < 1$.)

- The uncertainty in depth and camera translation can have a non-negligible effect on the *size* of R_1^*, however, when $\langle K_0 \rangle - 1 \ll 1$ and there is no overlap of R_0 and R. This is because for the lower choice (no overlap) in (38) the small quantity $(\langle K_0 \rangle - 1)\epsilon$ is multiplied by $\langle\omega_0\rangle$, which could be much larger than $\Delta\omega_0$. In the overlapping case (the upper choice), the same small quantity is multiplied only by $\Delta\omega_0$, and hence remains small compared to the first term.

- The effect on R_1^* of uncertainty in the position of the FOE and of F_0 is independent of how far away F_0 is from the FOE (in the case of no overlap). In contrast, the effect of the uncertainty in depth is a monotonically increasing function of the distance of F_0 from the FOE, owing to the presence of the $\langle\omega_0\rangle$ in the (lower choice) in (38).

4.2 Calculating depth from uncertainly known FOE, F_0, and F_1.

4.2.1 General results

We assume that the FOE and the positions p_0 and p_1 of the interest point F are known only to lie inside their respective uncertainty rectangles (see Figure 5). We will use the positions and sizes of these rectangles to calculate both the "best estimate" Z_1^{mean} for the environmental depth Z_1, and the uncertainty δZ_1 in this value. We have from (6) that

$$Z_1 = \frac{D_0}{\Delta D_0} T, \tag{39}$$

where D_0 and ΔD_0 are assumed to lie in the intervals

$$\begin{aligned} \langle D_0 \rangle - \delta D_0 \leq \quad & D_0 \quad \leq \langle D_0 \rangle + \delta D_0, \\ \langle \Delta D_0 \rangle - \delta(\Delta D_0) \leq \quad & \Delta D_0 \quad \leq \langle \Delta D_0 \rangle + \delta(\Delta D_0), \end{aligned} \tag{40}$$

and T is known accurately ($\delta T = 0$, $T = \langle \text{T} \rangle$). The latter assumption is made only for simplicity of exposition; the effect of uncertain T is easily included, but complicates the appearance of the formulas. We then use (39) to find the allowed range of values for Z_1:

$$Z_1^{\text{mean}} - \delta Z_1 \leq Z_1 \leq Z_1^{\text{mean}} + \delta Z_1.$$

To simplify the analysis, we first define the *relative uncertainty* α in D_0, and the *relative uncertainty* β in ΔD_0:

$$\alpha = \frac{\delta D_0}{\langle D_0 \rangle} \; ; \; \beta = \frac{\delta(\Delta D_0)}{\langle \Delta D_0 \rangle}. \tag{41}$$

We also define the nominal value $\langle Z_1 \rangle$ of Z_1 to be

$$\langle Z_1 \rangle = \frac{\langle D_0 \rangle}{\langle \Delta D \rangle_0} \langle T \rangle. \tag{42}$$

That is, $\langle Z_1 \rangle$ is just the value one would expect from (39) in the absence of uncertainty.

We then have that

$$
\begin{aligned}
Z_1^{\text{mean}} \pm \delta Z_1 &= \langle \mathrm{T} \rangle \cdot \frac{\langle \mathrm{D}_0 \rangle \pm \delta \mathrm{D}_0}{\langle \Delta \mathrm{D}_0 \rangle \mp \delta(\Delta \mathrm{D}_0)} \\
&= \langle Z_1 \rangle \cdot \frac{1 \pm \alpha}{1 \mp \beta}, \qquad (43)
\end{aligned}
$$

from which it follows that

$$
\begin{aligned}
Z_1^{\text{mean}} &= \langle Z_1 \rangle \cdot \frac{1 + \alpha\beta}{1 - \beta^2}, \qquad (44) \\
\delta Z_1 &= \langle Z_1 \rangle \cdot \frac{\alpha + \beta}{1 - \beta^2}. \qquad (45)
\end{aligned}
$$

Note that the "best" estimate Z_1^{mean} for Z_1 is not equal to the value $\langle Z_1 \rangle$ which would be obtained by substituting the best values for the other quantities into (39). Indeed, $Z_1^{\text{mean}} \geq \langle Z_1 \rangle$, equality holding only when $\beta = 0$, i.e., there is no uncertainty in ΔD_0. The relative uncertainty in Z_1 is, using (44) and (45), given by

$$
\frac{\delta Z_1}{Z_1^{\text{mean}}} = \frac{\alpha + \beta}{1 + \alpha\beta}. \qquad (46)
$$

We use the result (46) in Appendix B to give quantitative meaning to two well known results in motion analysis.

In practice, the relative uncertainty in inter–frame interest point displacements is often much larger than that in the distance of interest points from the FOE (see the end of this section). This is equivalent to neglecting α in (44) and (45). In this special case, we then have

$$Z_1^{\text{mean}} \cong \frac{\langle Z_1 \rangle}{1-\beta^2}, \tag{47}$$

$$\delta Z_1 \cong \beta Z_1^{\text{mean}}, \tag{48}$$

and hence the relative uncertainty in Z_1 is just equal to the relative uncertainty β in ΔD_0.

4.2.2 The calculation of the relative uncertainties α and β

We now calculate the relative uncertainties α and β in terms of the uncertainties in the position of the FOE, F_0 and F_1. Exact expressions for α and β can be derived for any disposition of the uncertainty rectangles R, R_0, and R_1 with respect to the nominal points $\langle$FOE$\rangle$, $\langle p_0 \rangle$, and $\langle p_1 \rangle$. The interested reader may confirm for herself that such expressions will generally be quite complicated, and hence computationally expensive. However, as mentioned in the introduction, finding an exact expression for a quantity which depends on imprecisely defined entities (such as uncertainty rectangles) is both unjustifiable and dangerous, since it lends an unwarranted air of precision to the quantity in question. We thus content ourselves with expressions for α and β which are good approximations for all but the most pathological cases, and have the added virtue of being extremely simple.

We make the following assumptions. We assume that the NDP passes through the nominal points $\langle$FOE$\rangle$, $\langle p_0 \rangle$, and $\langle p_1 \rangle$. We then calculate the relative uncertainties α and β in D_0 and ΔD_0 by restricting the possible positions of FOE, p_0, and p_1 to be along the NDP. The interested reader may confirm that the resultant approximate expressions for α and β are lower bounds on the exact expressions for α and β. Generally speaking, these approximate expressions will be good approximations to the exact expressions when

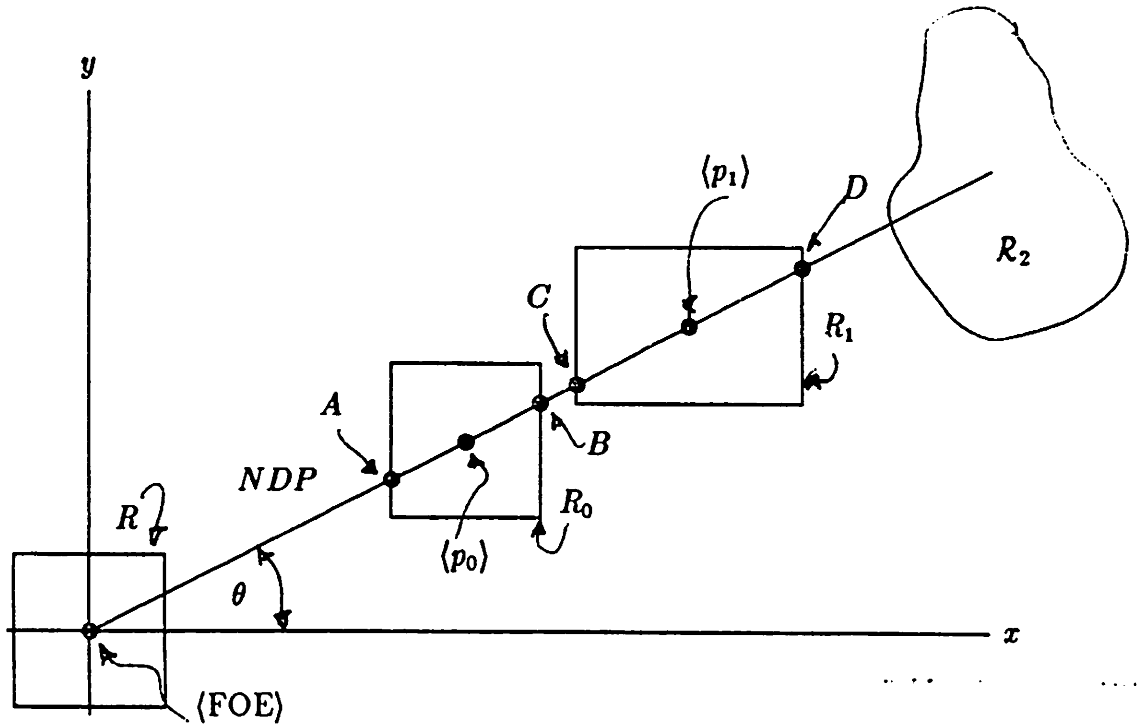

Figure 5: **Case VVV**: the NDP passes through the vertical sides of all the uncertainty rectangles

the nominal points do not lie very far off the NDP (which could, for instance, be obtained by a least–squares fit to ⟨FOE⟩, $\langle p_0 \rangle$, and $\langle p_1 \rangle$), and when the uncertainty rectangles are approximately square.

The reader should consult Appendix C for details of the calculation of α and β, and for definitions and notation; we give here only two examples. In the case VVV, the NDP passes through the vertical sides of the three uncertainty rectangles (see Figure 5). In the case HHH, the NDP passes through the horizontal sides of the three uncertainty rectangles (see Figure 6). It should be clear that the second case is identical to the first if we simply interchange x and y.

Algebraically, if the NDP passes through the center of each of the uncertainty rectan-

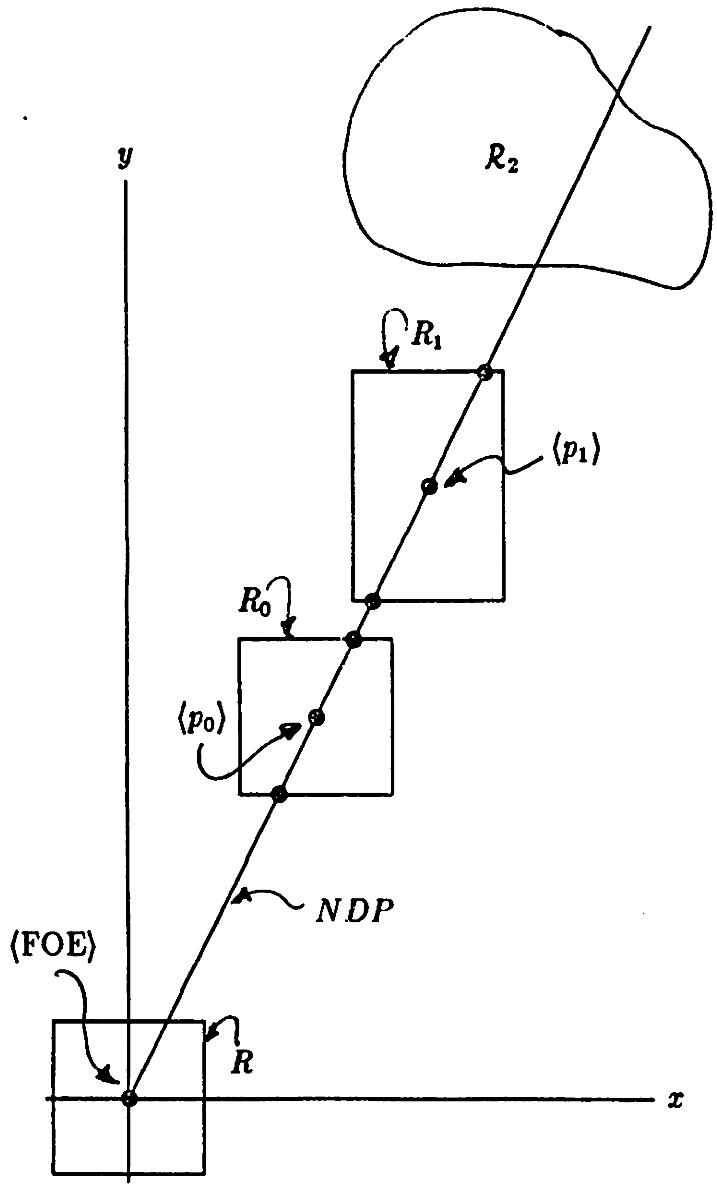

Figure 6: **Case HHH**: the NDP passes through the horizontal sides of the uncertainty rectangles

gles, the first and second cases are those for which

$$\frac{\Delta y}{\Delta x}, \ \frac{\Delta y_0}{\Delta x_0}, \ \frac{\Delta y_1}{\Delta x_1} \left\{ \begin{matrix} > \\ < \end{matrix} \right\} \frac{\langle y_0 \rangle}{\langle x_0 \rangle}, \tag{49}$$

where the upper choice is made for the first case, and the lower choice for the second case. The expressions for α and β when the NDP passes through the *vertical* sides of the uncertainty rectangles (case VVV) are then given by (see Appendix C)

$$\begin{aligned} \alpha &= \frac{\Delta x + \Delta x_0}{\langle x_0 \rangle}, \\ \beta &= \frac{\Delta x_0 + \Delta x_1}{\langle x_1 \rangle - \langle x_0 \rangle} \\ &= \left[\frac{1}{\langle K_0 \rangle - 1} \right] \frac{\Delta x_0 + \Delta x_1}{\langle x_0 \rangle} \\ &= \left[\frac{1}{\langle K_0 \rangle - 1} \right] \left[\frac{\Delta x_0 + \Delta x_1}{\Delta x + \Delta x_0} \right] \alpha, \end{aligned} \tag{50}$$

where we have used equation (9):

$$\langle x_1 \rangle = \langle K_0 \rangle \langle x_0 \rangle. \tag{51}$$

If the NDP passes through the *horizontal* sides of the rectangles (case HHH), the expressions for α and β are obtained by interchanging x and y in (50):

$$\begin{aligned} \alpha &= \frac{\Delta y + \Delta y_0}{\langle y_0 \rangle}, \\ \beta &= \frac{\Delta y_0 + \Delta y_1}{\langle y_1 \rangle - \langle y_0 \rangle} \\ &= \left[\frac{1}{\langle K_0 \rangle - 1} \right] \frac{\Delta y_0 + \Delta y_1}{\langle y_0 \rangle} \end{aligned}$$

$$= \left[\frac{1}{\langle K_0\rangle - 1}\right]\left[\frac{\Delta y_0 + \Delta y_1}{\Delta y + \Delta y_0}\right]\alpha, \tag{52}$$

We see from expressions (50) and (52) that when the camera translation is much smaller than the depth ($T \ll Z_0$), and the uncertainty in the position of the FOE is comparable to that in the positions of F_0 and F_1, the quantity β is much greater than the quantity α. The uncertainty in the position of the FOE thus has little effect on the computation of depth unless its uncertainty is much larger than that in F_0 and F_1 (for $T \ll Z_0$). In this case expressions (47) and (48) for Z_1^{mean} and δZ_1 will be good approximations. Similar conclusions can be drawn for the remaining six cases.

In the general case of arbitrarily shaped uncertainty regions, and of nominal points which do not lie on the NDP, the calculation of α and β is correspondingly more complicated. But as a rough approximation, we can generalize the expressions we have found for α and β as follows. Let the segment of the NDP intersected by R have length $2d$, that intersected by R_0 have length $2d_0$, and that intersected by R_1 have length $2d_1$ (see Figure 7). Let $\langle D_0\rangle$ and $\langle D_1\rangle$ be the distances from the origin of the coördinate system to p_0 and p_1, respectively. Then one easily convinces oneself that an approximation to α and β is furnished by

$$\alpha \cong \frac{d + d_0}{\langle D_0\rangle} \tag{53}$$

$$\beta \cong \frac{d_0 + d_1}{\langle D_1\rangle - \langle D_0\rangle} \tag{54}$$

$$\cong \left[\frac{1}{\langle K_0\rangle - 1}\right]\left[\frac{d_0 + d_1}{\langle D_0\rangle}\right] \tag{55}$$

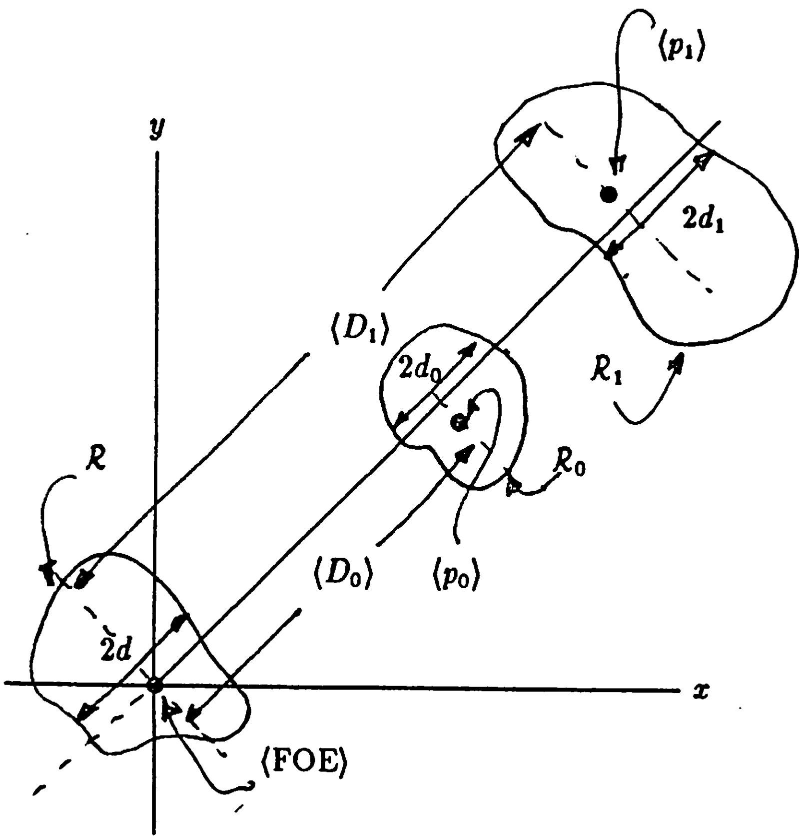

Figure 7: A general set of uncertainty regions, with approximate values for the uncertainties in the position of the nominal points.

$$\cong \left[\frac{1}{\langle K_0\rangle - 1}\right]\left[\frac{d_0+d_1}{d_0+d}\right]\alpha \tag{56}$$

We see from this analysis that the following qualitative conclusions may be drawn:

- When the inter-frame camera translation is small compared to the depth ($T \ll Z_0$), the uncertainty in inter-frame image displacements is the most significant contribution to the calculation of the uncertainty in depth; the uncertainty in the distances of image points from the FOE is less significant.

- When $T \ll Z_0$, the uncertainty in the FOE has little effect on the computation of the uncertainty in depth, unless the uncertainty in the FOE is large compared to that in F_0 and F_1.

4.3 Calculating the search region $\mathcal{R}_2$ for F_2 from uncertainly known FOE, F_0, and F_1.

The task of this section is to find the search region for the interest point F in the third frame, frame 2. We could analyze this situation *de novo*, but that is not necessary. In Section 4.1 we found the effect an uncertain value for Z_0, and uncertain positions for the FOE and p_0, had on the search region for p_1. In the case at hand, we have an uncertain value for Z_1 which follows from uncertain positions for the FOE, F_0, and F_1. Strictly speaking, this is a difficult problem to analyze, but an approximate solution can be found in the following way.

- Find the uncertainty in Z_1 from the uncertainty in the FOE, F_0, and F_1, using the appropriate results of Appendix C.

- Ignore the point F_0, treat F_1 as a new "initial" frame, and use the results of Section 4.1.2.

The result is that one makes the replacements in the results of Section 4.1.2 (summarized in Appendix D):

$$\langle K_0 \rangle \Rightarrow K_1^{\text{mean}} \tag{57}$$

$$\langle Z_0 \rangle \Rightarrow Z_1^{\text{mean}} \tag{58}$$

$$\text{any "0" subscript} \Rightarrow \text{a "1" subscript}, \tag{59}$$

where

$$K_1^{\text{mean}} = \frac{Z_1^{\text{mean}}}{Z_1^{\text{mean}} - \langle T \rangle}, \tag{60}$$

and Z_1^{mean} is given by (44), δZ_1 by (45), and α and β by the results of Appendix C. The details of this replacement are given in Appendix D.

5 Some examples of the technique

In this section we give some examples of the results derived in Section 4 and summarized in Appendix D.

5.1 Search regions for F_1 for uncertain depth (non–overlapping case)

In the following three tables, we give, for the non–overlapping case, the sides of the search rectangle R_1^* for various values of $\langle T \rangle / \langle Z_0 \rangle$, various sizes of the uncertainty rectangles for the FOE and F_0, for relative uncertainty in depth of 10% and 20%, and no uncertainty in the inter-frame camera translation. We assume that $\langle x_0 \rangle = \langle y_0 \rangle = 50$. The relevant equations are the expressions for S_x and S_y in Section 4.1, equation (38), which are summarized in Case II.1 of the Summary (Appendix D). Remember that the actual search region is the intersection of a "wedge" with the rectangle R_1^*. The column labels have the following meanings: R is the size of the uncertainty rectangle R, R_0 is the size of the uncertainty rectangle R_0, FOE is the contribution $(= 2\,(\langle K_0 \rangle - 1)\,\Delta x)$ of the uncertainty in the FOE to the side of the search rectangle, F_0 is the contribution $(= 2\langle K_0 \rangle \Delta x_0)$ of the uncertainty in F_0 to the side of the search rectangle, $X\,\%$ is the contribution $(= 2\langle K_0 \rangle\,(\langle K_0 \rangle - 1)\,[\delta Z_0/\langle Z_0 \rangle]\,\{\langle x_0 \rangle\})$ of an $X\,\%$ uncertainty in the depth Z_0 to the side of the search rectangle, Σ_0 is the sum of FOE and F_0 (no depth uncertainty), and Σ_X is the sum of FOE, F_0, and $X\,\%$. Note that the effect of the depth uncertainty on the horizontal side of the search rectangle R_1^* is proportional to the nominal x-coördinate of F_0, i.e., if $\langle x_0 \rangle$ were 100, instead of 50, then all the entries in the "$X\,\%$" columns in the tables would be doubled.

Table 1: $\langle \mathrm{T} \rangle = 0.01\,\langle \mathrm{Z}_0 \rangle\ (\langle K_0 \rangle = 1.01)$

Size		Contribution to Side of R_1^*				Side of R_1^*		
R	R_0	FOE	F_0	10 %	20 %	Σ_0	Σ_{10}	Σ_{20}
1 × 1	1 × 1	0.01	1.01	0.05	0.10	1.02	1.07	1.12
1 × 1	5 × 5	0.01	5.05	0.05	0.10	5.06	5.11	5.16
2 × 2	5 × 5	0.02	5.05	0.05	0.10	5.07	5.12	5.17
5 × 5	2 × 2	0.05	2.02	0.05	0.10	2.07	2.12	2.17
10 × 10	5 × 5	0.10	5.05	0.05	0.10	5.15	5.20	5.25

Table 2: $\langle T \rangle = 0.10 \langle Z_0 \rangle$ ($\langle K_0 \rangle = 1.11$)

Size		Contribution to Side of R_1^*				Side of R_1^*		
R	R_0	FOE	F_0	10 %	20 %	Σ_0	Σ_{10}	Σ_{20}
1 × 1	1 × 1	0.11	1.11	0.56	1.12	1.22	1.78	2.34
1 × 1	5 × 5	0.11	5.55	0.56	1.12	5.66	6.21	6.78
2 × 2	5 × 5	0.22	5.55	0.56	1.12	5.77	6.33	6.89
5 × 5	2 × 2	0.55	2.22	0.56	1.12	2.77	3.33	3.89
10 × 10	5 × 5	1.11	5.55	0.56	1.12	6.66	7.22	7.78

Table 3: $\langle T \rangle = 0.20 \langle Z_0 \rangle$ ($\langle K_0 \rangle = 1.25$)

Size		Contribution to Side of R_1^*				Side of R_1^*		
R	R_0	FOE	F_0	10 %	20 %	Σ_0	Σ_{10}	Σ_{20}
1 × 1	1 × 1	0.25	1.25	1.56	3.12	1.50	3.06	4.62
1 × 1	5 × 5	0.25	6.25	1.56	3.12	6.05	8.06	9.62
2 × 2	5 × 5	0.50	6.25	1.56	3.12	6.75	8.31	9.87
5 × 5	2 × 2	1.25	2.50	1.56	3.12	3.75	5.31	6.87
10 × 10	5 × 5	2.50	6.25	1.56	3.12	8.75	10.31	11.87

We see that the comments at the end of Section 4.1 are borne out in these examples:

- The contribution of the uncertainty in the position of the FOE does not have a large effect on the size of the search rectangle R_1^* unless the inter–frame camera translation is a significant fraction of the depth (say about 0.2 or greater) and the size of the FOE's uncertainty region is large. For instance, in the last row of the first table (for which $\langle T \rangle / \langle Z_0 \rangle = 0.01$) the rather large 10 × 10 uncertainty in the FOE contributes only about 2 % of the total uncertainty in F_1 (0.1 pixel out of 5.15 pixel). On the other hand, for the same row of the third table (for which $\langle T \rangle / \langle Z_0 \rangle = 0.2$; the camera translation is 20 times greater than in the first table), the same uncertainty in the FOE contributes about 28 % of the total uncertainty (2.5 pixels out of 8.75)

- The uncertainty in the depth can have a non-negligible effect on the search rectangle even if the inter-frame camera translation is small. For instance, in the first row of the first table (for $\langle \mathrm{T} \rangle / \langle \mathrm{Z}_0 \rangle = 0.01$), a 20 % uncertainty in the depth contributes about 9 % to the total uncertainty in the depth (0.1 pixel out of 1.12). This fraction would be almost doubled if $\langle x_0 \rangle$ were 100 instead of 50. For large $\langle \mathrm{T} \rangle / \langle \mathrm{Z}_0 \rangle$ the effect is more pronounced: in the last row of the third table ($\langle \mathrm{T} \rangle / \langle \mathrm{Z}_0 \rangle = 0.2$), the depth uncertainty contributes about 26 % of the uncertainty in R_1^*, which would be raised to 40 % if $\langle x_0 \rangle$ were 100 instead of 50.

5.2 Search rectangles for F_1 for uncertain depth (overlapping case)

In this section, we give an example of the search region when there is overlap on the x-axis. We will take

$$\begin{aligned} \langle \mathrm{T} \rangle &= 0.1 \langle Z_0 \rangle \\ \Delta x = \Delta y &= 10 \\ \Delta x_0 = \Delta y_0 &= 5 \\ \langle x_0 \rangle &= 10 \\ \langle y_0 \rangle &= 50. \end{aligned}$$

Since $\langle x_0 \rangle = 10 < 10 + 5 = \Delta x + \Delta x_0$, there is overlap on the x-axis. There is no overlap on the y-axis, so we can use the results of Appendix D, case II.3. We assume there is an uncertainty of 10 % in Z_0. We then find:

$$C_x = 11.23$$

$$C_y = 55.73$$

$$S_x = 8.49$$

$$S_y = 12.77$$

and

$$x^{\max}(y) = -\frac{1}{7}y + 11.43$$

$$x^{\min}(y) = +\frac{5}{7}y - 17.14\,.$$

We can then find the search region $\mathcal{R}_1$ and compare this to the approximate search region, the rectangle R_1^* described above (see Figure 8). We find that the area of the search region is about 322 pixels, whereas the area of the rectangle is about 434 pixels. Consequently, by using the rectangle rather than the exact search region, we will "oversearch" by $434 - 322 = 112$ pixels. This is about 35 % of the exact search region. On the other hand, calculation of the exact search region and its implementation may involve a fair amount of computation. Since, in this example at least, using the more easily found search rectangle rather than the exact search region does not lead to a huge increase in computation, it may be more efficient to search the rectangular region R_1^* rather than the exact search region $\mathcal{R}_1$.

6 Summary and Conclusions

We have attempted to outline a general approach to the calculation of uncertainties in environmental parameters. We considered as an example the calculation of environmental depth from motion, although similar considerations could be applied to stereo, or to the calculation of other environmental parameters, such as object rotational and translational

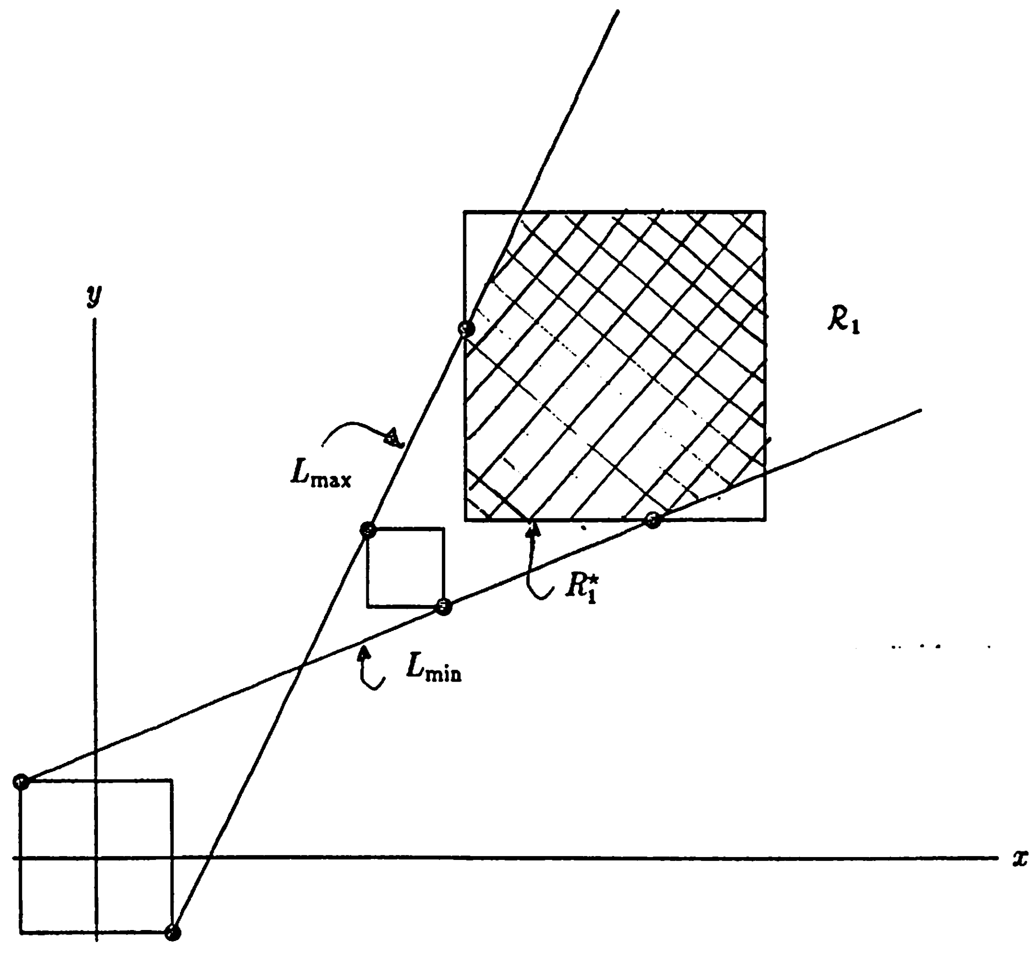

Figure 8: The search region $\mathcal{R}_1$. The shaded region $\mathcal{R}_1$ is the intersection of the search rectangle R_1^* with the "wedge" lying below L_{max} and above L_{min}.

velocities. In future work we will apply these techniques to analyze the accuracy with which motion parameters can be determined from image quantities and to analyze the relative accuracy of stereo and motion techniques. We will also investigate the implications of uncertainty analysis for the multi-frame technique of [Bhar1985].

6.1 Qualitative summary of quantitative results

We summarize here in a qualitative way some of the quantitative results of this paper.

- The uncertainty in the FOE is important, in general, for calculating search regions or depth only when the uncertainty region for the FOE is large compared to those of the image points, or when the inter-frame camera translation is a significant fraction of the depth.
- When the inter-frame camera translation is small compared to the depth ($T \ll Z$) the uncertainty in the FOE has little effect on the search regions or the calculation of depth, compared to the effect of the uncertainty in the position of image points.
- When $T \ll Z$ the uncertainty in the depth *can* have a significant effect on search regions, especially for image points which are far from the FOE.
- When the inter-frame camera translation is *not* small compared to the depth, all uncertainties are important.

Acknowledgements

I thank Prof. E. Riseman for his advice and encouragement, and for his careful reading of the manuscript. I would also like to thank P. Anandan and P. Kahn for extensive discussions of this work, and I. Pavlin for critically reading an earlier version. Comments made by L. Kitchen and D. Strahman led to improvements in the manuscript.

References

[Bhar1985] S. Bharwani, E. Riseman, and A. Hanson, "Refinement of environmental depth maps over multiple frames," DARPA I. U. Workshop Proc., Dec. 1985.

[Kitc1982] L. Kitchen and A. Rosenfeld, "Grey-level corner detection," Patt. Rec. Lett. **1** (1982), 95–102.

[Lawt1984] D. T. Lawton, "Processing dynamic image sequences from a moving sensor," Ph.D. Thesis, COINS Dept., U. Mass, Amherst, MA , Tech. Rep. 84-05 (1984).

[Long1980] H. C. Longuet-Higgins and K. Prazdny, "The interpretation of a moving retinal image," *Proc. Roy. Soc. Lon.* **B208** (1980), 385-397.

[Mora1980] H. P. Moravec, "Obstacle avoidance and navigation in the real world by a seeing robot," Ph.D. Thesis, SAIL, Stanford, Cal. (Sept. 1980).

[Waxm1985a] A. M. Waxman, et al., "Image processing for visual navigation of a roadway," U. Maryland CAR Tech. Rep. #138 (1985).

[Waxm1985b] A. M. Waxman, et al., "A visual navigation system for the Autonomous Land Vehicle, " U. Maryland CAR Tech. Rep. #139, July 1985.

A The search region $\mathcal{R}_1$

Here we find the exact form for the search region $\mathcal{R}_1$ considered in Section 4.2. We must distinguish two cases: the case where the projections of R and R_0 onto the coördinate axes do not overlap, and the case where they do. We consider the non–overlapping case in A.1, and the overlapping case in A.2.

A.1 The non–overlapping case

The case where the projections of R and R_0 onto the coördinate axes do not overlap corresponds algebraically to the requirements

$$\begin{aligned} \langle x_0 \rangle &> \Delta x + \Delta x_0 \\ \langle y_0 \rangle &> \Delta y + \Delta y_0 \end{aligned}$$

This situation is shown in Figure 9. In this figure, we show the search rectangle $R_1(K_0)$ for a particular value of K_0. According to the analysis of Section 4.1.2, we want to find the union of all such rectangles for values of K_0 in some interval I. We show that the points A, B, and E lie on a straight line L_{max}, and that the points C, D, and F lie on a straight line L_{min}, and that these lines are independent of the value of K_0. The search region $\mathcal{R}_1$ will then be the intersection of the "wedge" lying below L_{max} and above L_{min} with the rectangle R_1^* described in Section 4.1.2 (see Figure 8). Note that L_{max} (L_{min}) is the line of maximum (minimum) slope among all lines passing through R and R_0.

The coördinates of each of these points are given by

$$\left\{ \begin{array}{c} A \\ C \end{array} \right\} = (\pm\Delta x, \mp\Delta y) \tag{61}$$

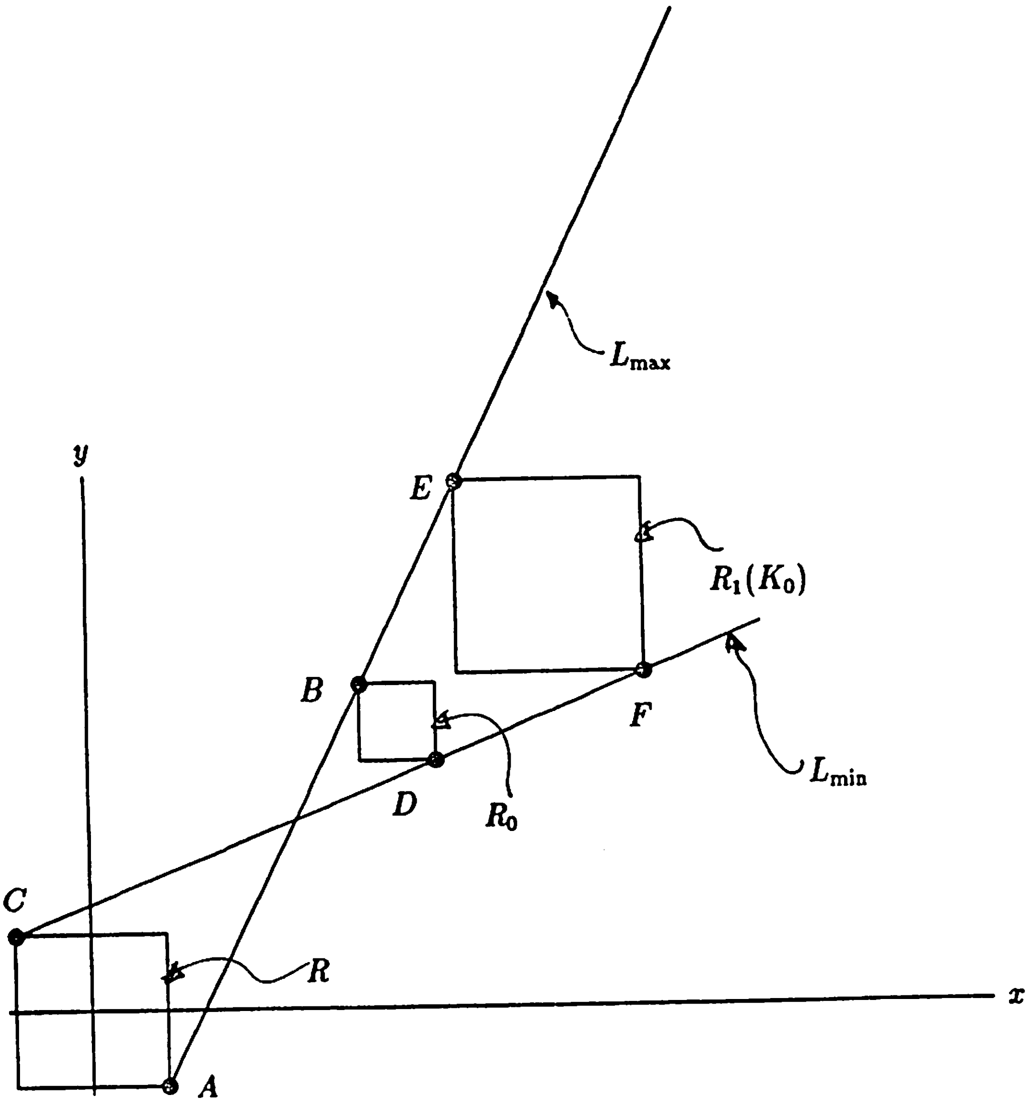

Figure 9: The search rectangle $R_1(K_0)$ in the non-overlapping case

$$\left\{\begin{matrix} B \\ D \end{matrix}\right\} = (\langle x_0\rangle \mp \Delta x_0, \langle y_0\rangle \pm \Delta y_0) \tag{62}$$

$$\left\{\begin{matrix} E \\ F \end{matrix}\right\} = (K_0\langle x_0\rangle \mp (K_0\Delta x_0 + (K_0 - 1)\Delta x)\,, K_0\langle y_0\rangle \pm (K_0\Delta y_0 + (K_0 - 1)\Delta y))\ . \tag{63}$$

The points A, B, and E lie along a line $L_{\max}$ if and only if

$$\frac{y_{\mathrm{E}} - y_{\mathrm{B}}}{x_{\mathrm{E}} - x_{\mathrm{B}}} = \frac{y_{\mathrm{B}} - y_{\mathrm{A}}}{x_{\mathrm{B}} - x_{\mathrm{A}}}, \tag{64}$$

and the points C, D, and F lie along a line $L_{\min}$ if and only if

$$\frac{y_{\mathrm{F}} - y_{\mathrm{D}}}{x_{\mathrm{F}} - x_{\mathrm{D}}} = \frac{y_{\mathrm{D}} - y_{\mathrm{C}}}{x_{\mathrm{D}} - x_{\mathrm{C}}}. \tag{65}$$

We may prove both of these simultaneously. Using the upper (lower) sign to correspond to (64)((65)), we want to show that

$$\frac{[K_0\langle y_0\rangle \pm (K_0\Delta y_0 + (K_0 - 1)\Delta y)] - (\langle y_0\rangle \pm \Delta y_0)}{[K_0\langle x_0\rangle \mp (K_0\Delta x_0 + (K_0 - 1)\Delta x)] - (\langle x_0\rangle \mp \Delta x_0)} = \frac{(\langle y_0\rangle \pm \Delta y_0) - (\mp\Delta y)}{(\langle x_0\rangle \mp \Delta x_0) - (\pm\Delta x)}. \tag{66}$$

But the left-hand-side of (66) is just

$$\frac{(K_0 - 1)\,[\langle y_0\rangle \pm (\Delta y + \Delta y_0)]}{(K_0 - 1)\,[\langle x_0\rangle \mp (\Delta x + \Delta x_0)]} = \frac{\langle y_0\rangle \pm (\Delta y + \Delta y_0)}{\langle x_0\rangle \mp (\Delta x + \Delta x_0)}, \tag{67}$$

Q.E.D.

Thus, A, B, and E lie on the line $L_{\max}$ and C, D, and F lie on the line $L_{\min}$. Since this is true for arbitrary K_0, it follows that all the upper left-hand corners ("E") of all the $R_1(K_0)$ lie on the line $L_{\max}$, and all the lower right-hand corners ("F") of all the $R_1(K_0)$ lie on the line $L_{\min}$. It is then obvious that $\mathcal{R}_1$ is the intersection of the rectangle R_1^*

given by equations (33) and (34) with the lower choice (since this corresponds to the "no overlap" case) in equations (37) and (38) with the wedge–like region between the lines $L_{\max}$ and $L_{\min}$.

The equations of these lines can be easily found by substituting the coördinates (x, y) of an arbitrary point on either line for the coördinates of E or F. With the same notational convention as before, we find that the equation of $L_{\max}$ ($L_{\min}$) is given by

$$\frac{y - (\langle y_0 \rangle \pm \Delta y_0)}{x - (\langle x_0 \rangle \mp \Delta x_0)} = \frac{(\langle y_0 \rangle \pm \Delta y_0) - (\mp \Delta y)}{(\langle x_0 \rangle \mp \Delta x_0) - (\pm \Delta x)}, \tag{68}$$

which upon simplification becomes

$$y_{\min}^{\max}(x) = (x \mp \Delta x) \left[\frac{\langle y_0 \rangle \pm (\Delta y + \Delta y_0)}{\langle x_0 \rangle \mp (\Delta x + \Delta x_0)} \right] \mp \Delta y, \tag{69}$$

where we have denoted the equation for $L_{\max}$ by $y_{\max}(x)$ and that for $L_{\min}$ by $y_{\min}(x)$. the wedge is then defined as the locus of all points (x, y) satisfying

$$y_{\min}(x) \leq y \leq y_{\max}(x). \tag{70}$$

In summary, when the projections of R and R_0 onto the coördinate axes do not overlap the search region R_1 is the intersection of the wedge given by (70) and the rectangle R_1^* given by (33) and (34), with the lower choice in (37) and (38).

A.2 The overlapping case

We now consider the case in which the projections of R and R_0 onto one of the coördinate axes overlap. We consider only the case where the overlap is on the y–axis, i.e., where

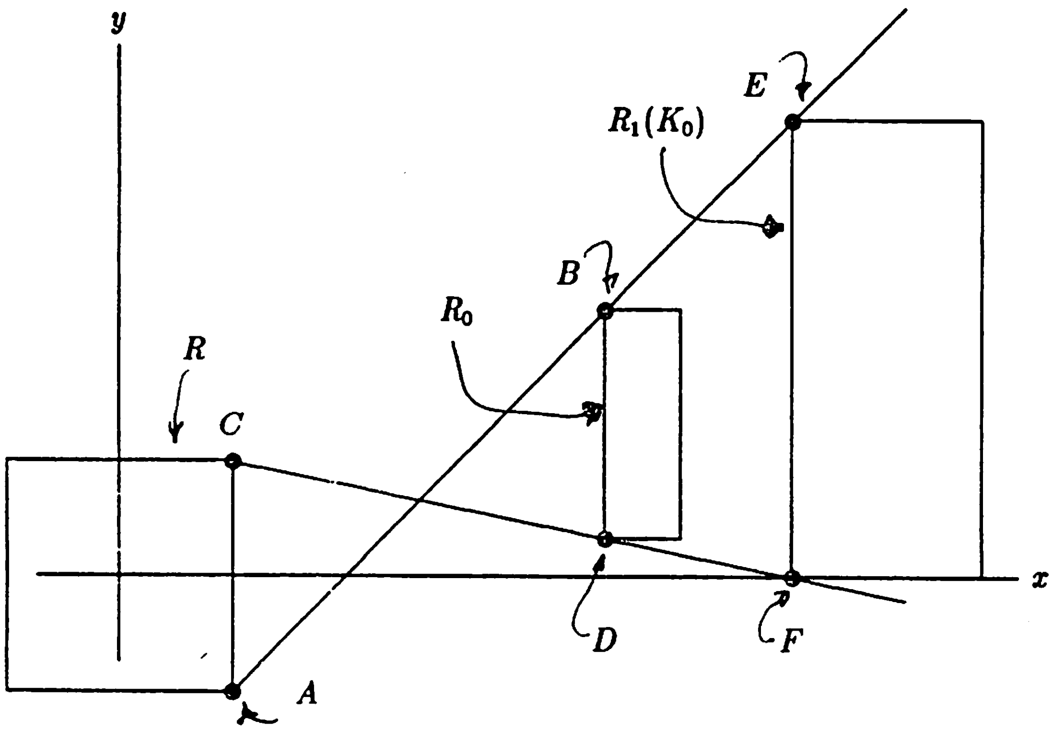

Figure 10: The search rectangle $R_1(K_0)$ in the case of overlapping along the y-axis

$\langle y_0 \rangle < \Delta y + \Delta y_0$, since the case of overlap on the x-axis is identical to this, except that the roles of y and x are interchanged.

The geometry of this situation is given in Figure 10. The coördinates of the points shown are easily seen to be

$$\left\{ \begin{array}{c} A \\ C \end{array} \right\} = (\Delta x, \mp \Delta y) \tag{71}$$

$$\left\{ \begin{array}{c} B \\ D \end{array} \right\} = (\langle x_0 \rangle - \Delta x_0, \langle y_0 \rangle \pm \Delta y_0) \tag{72}$$

$$\left\{ \begin{array}{c} E \\ F \end{array} \right\} = (K_0 \langle x_0 \rangle - (K_0 \Delta x_0 + (K_0 - 1)\Delta x)\,, K_0 \langle y_0 \rangle \pm (K_0 \Delta y_0 + (K_0 - 1)\Delta y))\ . \tag{73}$$

Using a method identical to that of the previous section, one can easily show that A,

B, and E are on a line $L_{\max}$, and that C, D, and F are on a line $L_{\min}$, for arbitrary K_0. Consequently, the search region $\mathcal{R}_1$ is the intersection of the rectangle R_1^* with the "wedge" lying between these two lines. As in the previous section, $L_{\max}$ and $L_{\min}$ are the lines of maximum and minimum slope, respectively, of all lines passing through R and R_0. The equations of $L_{\max}$ and $L_{\min}$ are then easily found to be

$$y_{\min}^{\max}(x) = (x - \Delta x)\left[\frac{\langle y_0\rangle \mp (\Delta y + \Delta y_0)}{\langle x_0\rangle - (\Delta x + \Delta x_0)}\right] \pm \Delta y, \tag{74}$$

respectively. The wedge is thus described algebraically by equation (70), with $y^{\max}(x)$ and $y_{\min}(x)$ given by (74).

The rectangle R_1^* is then in this case given by (33) and (34), with C_x (C_y) given by the lower (upper) choice in (37), and S_x (S_y) given by the lower (upper) choice in (38),i.e.,

$$C_x = \langle K_0\rangle\langle x_0\rangle\left\{1 + (\langle K_0\rangle - 1)\,[\epsilon]\left[\frac{\Delta x + \Delta x_0}{\langle x_0\rangle}\right]\right\}, \tag{75}$$

$$C_y = \langle K_0\rangle\langle y_0\rangle\left\{1 + (\langle K_0\rangle - 1)\,[\epsilon]\right\}, \tag{76}$$

$$S_x = \langle K_0\rangle\Delta x_0 + (\langle K_0\rangle - 1)\Delta x + \langle K_0\rangle(\langle K_0\rangle - 1)[\epsilon]\left\{\langle x_0\rangle\right\}, \tag{77}$$

$$S_y = \langle K_0\rangle\Delta y_0 + (\langle K_0\rangle - 1)\Delta y + \langle K_0\rangle(\langle K_0\rangle - 1)[\epsilon]\left\{\Delta y + \Delta y_0\right\}. \tag{78}$$

B When are depth calculations unreliable?

We show how equation (46) can be used to give quantitative justification and meaning to two well known "rules of thumb" in motion research.

Part of the "folklore" of motion research is that depth estimates are unreliable in two situations:

- When the interest point is "close" to the FOE

- When the environmental correlate to the interest point is "far away" from the camera.

To our knowledge a quantitative justification for these two statements has never been given. We propose to do that here.

The important equations that we will use are (46), (53), (54), and (55). From (46) we see that the relative uncertainty in the depth is large (the depth estimate is unreliable) whenever either α or β is "large" (here and in the following "large" means "large as a fraction"), i.e., either is comparable to 1 in value.

The quantity α will be large in this sense, following (53), whenever $d + d_0$ is comparable to $\langle D_0 \rangle$. This is most likely to occur when the interest point is "close" to the FOE. The point here, though, is that (53) gives "close" a precise meaning: a point is close to the FOE if $d + d_0$ is comparable to $\langle D_0 \rangle$.

The quantity β will be large, following (54), whenever $d_0 + d_1$ is comparable to $\langle D_1 \rangle - \langle D_0 \rangle$. Using equation (55), we see that this will be the case when either (1) the interest point is "close" to the FOE, where "close" means that $d_0 + d_1$ is comparable to $\langle D_0 \rangle$, or (2) the quantity $\langle K_0 \rangle - 1 \ll 1$. But using (25), we see that this means that $\langle \mathrm{T} \rangle \ll \langle \mathrm{Z}_0 \rangle$. That is, the environmental point is "far away" from the camera, where "far away" means that $\langle Z_0 \rangle \gg \langle \mathrm{T} \rangle$. We thus have given a quantitative justification and meaning to the two statements made at the beginning of this section. We summarize these as follows:

- The relative uncertainty in the depth is large when the interest point is "close" to the FOE, where by "close" is meant that either $d + d_0$ or $d_0 + d_1$ is comparable to $\langle D_0 \rangle$. A sufficient, but not necessary, condition for this is that d_0 is comparable to $\langle D_0 \rangle$, i.e.,

- When the interest point is "close" to the FOE

- When the environmental correlate to the interest point is "far away" from the camera.

To our knowledge a quantitative justification for these two statements has never been given. We propose to do that here.

The important equations that we will use are (46), (53), (54), and (55). From (46) we see that the relative uncertainty in the depth is large (the depth estimate is unreliable) whenever either α or β is "large" (here and in the following "large" means "large as a fraction"), i.e., either is comparable to 1 in value.

The quantity α will be large in this sense, following (53), whenever $d+d_0$ is comparable to $\langle D_0 \rangle$. This is most likely to occur when the interest point is "close" to the FOE. The point here, though, is that (53) gives "close" a precise meaning: a point is close to the FOE if $d+d_0$ is comparable to $\langle D_0 \rangle$.

The quantity β will be large, following (54), whenever d_0+d_1 is comparable to $\langle D_1 \rangle - \langle D_0 \rangle$. Using equation (55), we see that this will be the case when either (1) the interest point is "close" to the FOE, where "close" means that d_0+d_1 is comparable to $\langle D_0 \rangle$, or (2) the quantity $\langle K_0 \rangle - 1 \ll 1$. But using (25), we see that this means that $\langle \mathrm{T} \rangle \ll \langle \mathrm{Z}_0 \rangle$. That is, the environmental point is "far away" from the camera, where "far away" means that $\langle Z_0 \rangle \gg \langle \mathrm{T} \rangle$. We thus have given a quantitative justification and meaning to the two statements made at the beginning of this section. We summarize these as follows:

- The relative uncertainty in the depth is large when the interest point is "close" to the FOE, where by "close" is meant that either $d+d_0$ or d_0+d_1 is comparable to $\langle D_0 \rangle$. A sufficient, but not necessary, condition for this is that d_0 is comparable to $\langle D_0 \rangle$, i.e., the uncertainty in the position of the interest point is comparable to the distance of the interest point from the FOE.

- The relative uncertainty in the depth is large when the environmental correlate to the interest point is "far away" from the camera, where by "far away" is meant that $\langle Z_0 \rangle \gg \langle T \rangle$, i.e., the camera has moved between frames only a small fraction of the distance to the point.

We want to emphasize, however, that equation (46) enables one to *explicitly calculate* the uncertainty in the depth, and hence give quantitative meaning to the two comments given above.

C The calculation of α and β

In this section we calculate the relative uncertainties α and β in the distance of the interest point from the FOE, and in the inter-frame displacement of the interest point, respectively.

The calculation of α amounts to finding the maximum (minimum) distance D_{max} (D_{min}) between two points constrained so that one of the points lies in the uncertainty region R and the other point lies in the uncertainty region R_0. The calculation of β is identical to that for α, except that the two uncertainty regions are R_0 and R_1. We can thus compute α and β simultaneously by considering two uncertainty regions $\mathcal{R}$ and $\mathcal{R}'$. We define D_{max} (D_{min}) to be the maximum (minimum) distance between two points p and p' constrained so that $p \in \mathcal{R}$ and $p' \in \mathcal{R}'$:

$$D_{max} \equiv \max \{\langle pp' \rangle \mid p \in \mathcal{R},\ p' \in \mathcal{R}'\}, \tag{79}$$

$$D_{min} \equiv \min \{\langle pp' \rangle \mid p \in \mathcal{R},\ p' \in \mathcal{R}'\}, \tag{80}$$

where $\langle pp' \rangle$ is the distance between p and p'. We will refer to (79) and (80) as the *exact* extremum problem. If we write

$$D_{\max} = \langle D \rangle + \delta D, \quad (81)$$

$$D_{\min} = \langle D \rangle - \delta D, \quad (82)$$

then it follows that

$$\langle D \rangle = \frac{D_{\max} + D_{\min}}{2}, \quad (83)$$

$$\delta D = \frac{D_{\max} - D_{\min}}{2}. \quad (84)$$

The quantity α will then be determined by choosing $\mathcal{R} = R$, $\mathcal{R}' = R_0$, and β by choosing $\mathcal{R} = R_0$, $\mathcal{R}' = R_1$.

C.1 An approximate expression for α and β

The calculation of (79) and (80) can be performed easily for any disposition of the uncertainty rectangles with respect to the nominal displacement path, but it is cumbersome to display all the possible special cases, and the expressions will in general be quite complicated. However, as mentioned in the Introduction, a good approximation for $D_{\max}$ and $D_{\min}$ is all that is really desired, since the uncertainty rectangles are only approximately known anyway.

We thus replace the exact extremum problem represented by (79,80) by the following:

$$D_{\max} \equiv \max \{ \langle pp' \rangle \mid p \in \mathcal{R}, p \in NDP; \; p' \in \mathcal{R}', p' \in NDP \}, \quad (85)$$

$$D_{\min} \equiv \min \{ \langle pp' \rangle \mid p \in \mathcal{R}, p \in NDP; \; p' \in \mathcal{R}', p' \in NDP \}. \quad (86)$$

We also assume that the NDP passes through the center of each uncertainty rectangle. This new extremum problem corresponds to finding the minimum and maximum distance between two points constrained both to lie within their respective uncertainty rectangles *and* to lie along the nominal displacement path. We will refer to the calculation of (85,86) as the *restricted* extremum problem. We note that the values obtained for $D_{\max}$ ($D_{\min}$) for the restricted extremum problem are lower (upper) bounds for those of the exact extremum problem (79,80). This then implies, as the reader may show, that the quantities α and β derived from the restricted problem are lower bounds for the same quantities found in the exact problem. In almost all except the most pathological cases, however, the quantities derived for the restricted problem (85,86) are very good approximations to those for the exact problem (79,80).

The computation of (85,86) depends on how the NDP passes through each uncertainty rectangle. Let us call a side of a rectangle that is parallel to the x–axis a horizontal (H) side, and that which is parallel to the y–axis a vertical (V) side. Because the NDP is assumed to pass through the center of each of the uncertainty rectangles $\mathcal{R}$ and $\mathcal{R}'$, the NDP must pass either through both H–sides, or both V–sides, of each of the rectangles.[3] We denote the former situation by "H", and the latter by "V". There are thus four possible ways that the NDP can pass through the two rectangles. We denote each case by the symbol ij, where i and j can be either H or V. The first entry tells how the NDP passes through the rectangle $\mathcal{R}$ and the second entry tells how the NDP passes through $\mathcal{R}'$. The four cases are thus:

[3]It is of course possible that the NDP passes through two corners of the rectangle. This case can be considered either an H or a V–either will give the same results. We thus do not consider this to be a separate case.

Case VV The NDP passes through the V–side of $\mathcal{R}$ and the V–side of $\mathcal{R}'$ (Fig. 11).

Case HV The NDP passes through the H–side of $\mathcal{R}$ and the V–side of $\mathcal{R}'$ (Fig. 12).

Case VH The NDP passes through the V–side of $\mathcal{R}$ and the H–side of $\mathcal{R}'$ (Fig. 13).

Case HH The NDP passes through the H–side of $\mathcal{R}$ and the H–side of $\mathcal{R}'$ (Fig. 14).

In Figures 11–14, $\mathcal{R}$ is centered at

$$(\langle\xi\rangle, \langle\eta\rangle), \tag{87}$$

and has sides

$$\{2\Delta\xi, 2\Delta\eta\}, \tag{88}$$

while $\mathcal{R}'$ is centered at

$$(\langle\xi'\rangle, \langle\eta'\rangle), \tag{89}$$

and has sides

$$\{2\Delta\xi', 2\Delta\eta'\}. \tag{90}$$

The analytical condition for when the NDP passes through the H– or through the V–side of $\mathcal{R}$ is

$$\frac{\Delta\eta}{\Delta\xi} \left\{ \begin{matrix} > \\ < \end{matrix} \right\} m, \tag{91}$$

where m is the slope of the NDP, and where the upper sign is the condition that the NDP passes through the H–side of $\mathcal{R}$, and the lower sign the condition that it passes through the V–side. A similar expression holds for $\mathcal{R}'$:

$$\frac{\Delta\eta'}{\Delta\xi'} \left\{ \begin{matrix} > \\ < \end{matrix} \right\} m, \tag{92}$$

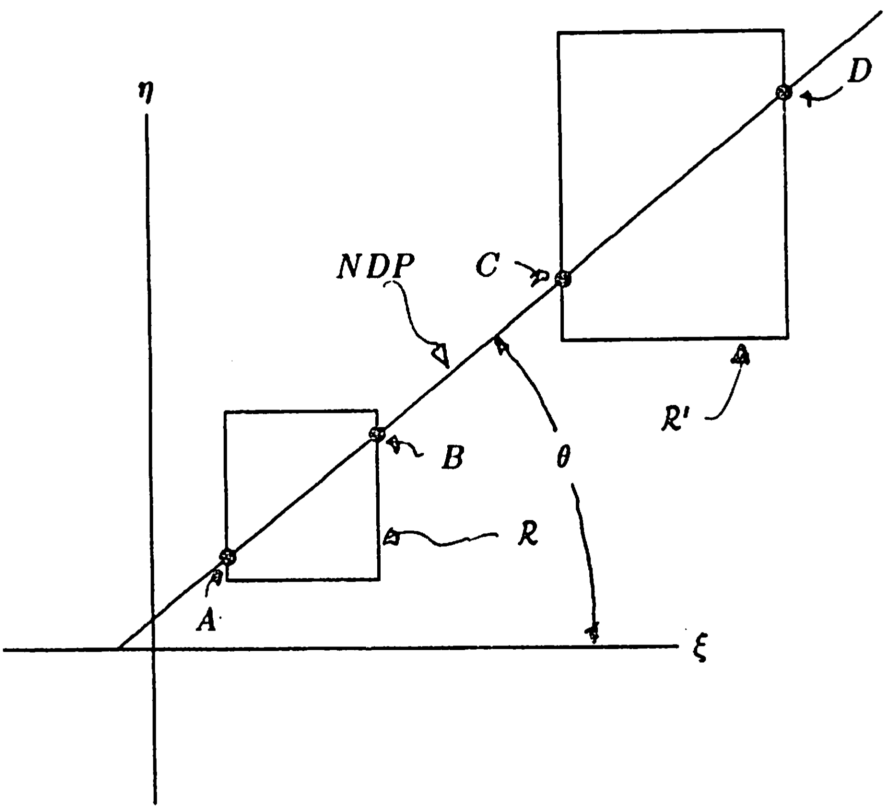

Figure 11: **Case VV:** the NDP passes through the vertical side of $\mathcal{R}$ and the vertical side of $\mathcal{R}'$.

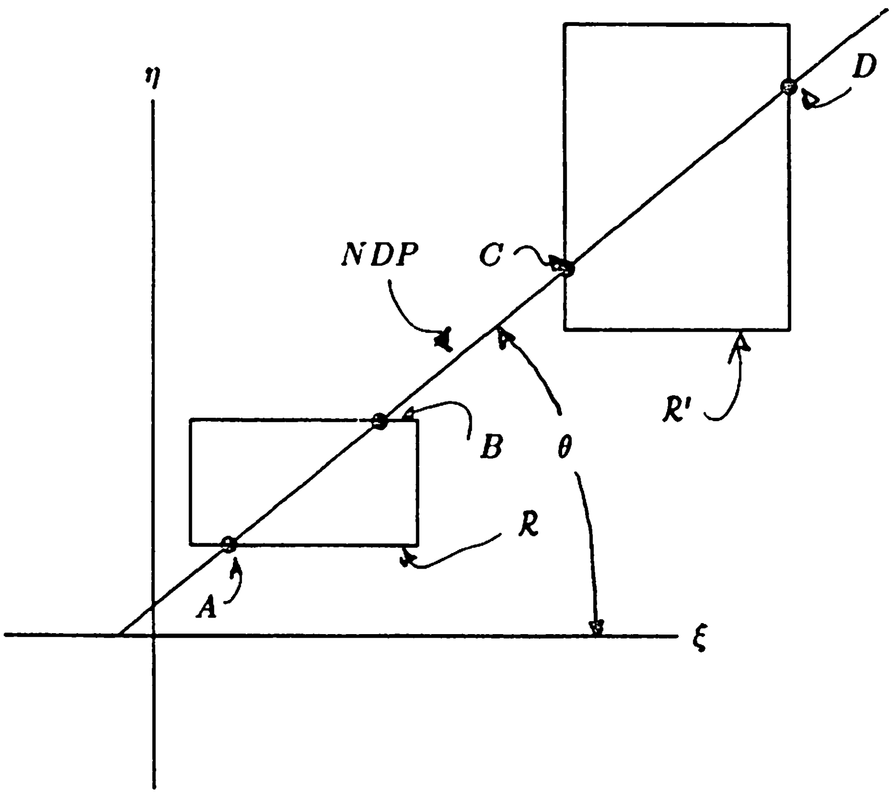

Figure 12: **Case HV:** the NDP passes through the horizontal side of $\mathcal{R}$ and the vertical side of $\mathcal{R}'$.

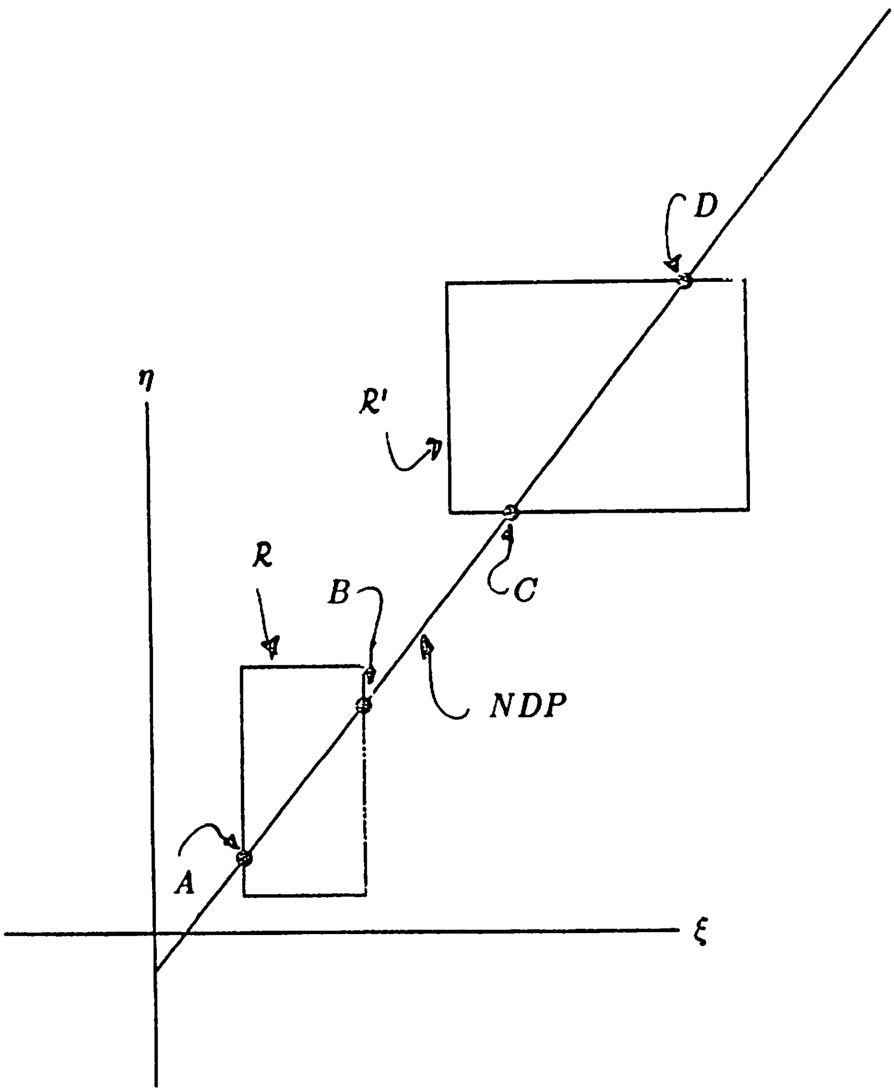

Figure 13: **Case VH:** the NDP passes through the vertical side of $\mathcal{R}$ and the horizontal side of $\mathcal{R}'$.

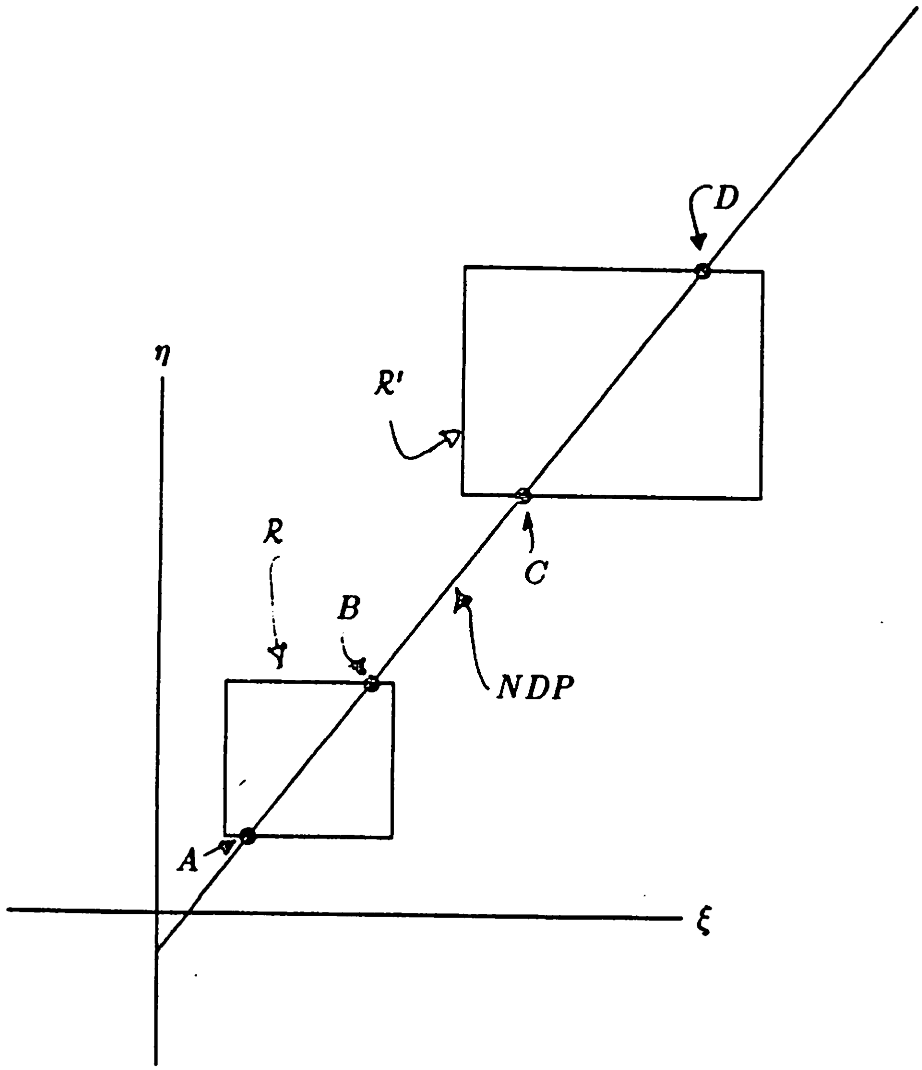

Figure 14: **Case HH:** the NDP passes through the horizontal side of $\mathcal{R}$ and the horizontal side of $\mathcal{R}'$.

with the same notation as in (91). Note that m is not primed in (92)

It should be clear from Figures 11–14 that we really only have to consider two of the four cases, namely case VV and case HV. This is because case HH is obtained from case VV by interchanging η and ξ (as is easily seen by flipping Figure 11 around the line $\eta = \xi$; this gives the graph for case HH, i.e., Figure 14). Identical comments hold for case VH, which is obtained from case HV by interchanging η and ξ.

In case VV, we find from Figure 11

$$D_{\max} = \mathrm{AD} = \frac{\langle\xi'\rangle - \langle\xi\rangle + (\Delta\xi + \Delta\xi')}{\cos\theta} \tag{93}$$

$$D_{\min} = \mathrm{BC} = \frac{\langle\xi'\rangle - \langle\xi\rangle - (\Delta\xi + \Delta\xi')}{\cos\theta}. \tag{94}$$

Hence, using (83) and (84) we see that

$$\delta D = \frac{\mathrm{AD} - \mathrm{BC}}{2} = \frac{\Delta\xi + \Delta\xi'}{\cos\theta},$$

$$\langle D\rangle = \frac{\mathrm{AD} + \mathrm{BC}}{2} = \frac{\langle\xi'\rangle - \langle\xi\rangle}{\cos\theta}.$$

Hence, in case VV, we have

$$\left(\frac{\delta D}{\langle D\rangle}\right)_{\mathrm{VV}} = \frac{\Delta\xi + \Delta\xi'}{\langle\xi'\rangle - \langle\xi\rangle}. \tag{95}$$

If we now consider case HV, we find from Figure 12 that

$$D_{\max} = \mathrm{AD} = \frac{\langle\xi'\rangle - \langle\xi\rangle}{\cos\theta} + \left\{\frac{\Delta\eta}{\sin\theta} + \frac{\Delta\xi'}{\cos\theta}\right\},$$

$$D_{\min} = \mathrm{BC} = \frac{\langle\xi'\rangle - \langle\xi\rangle}{\cos\theta} - \left\{\frac{\Delta\eta}{\sin\theta} + \frac{\Delta\xi'}{\cos\theta}\right\}.$$

We then have

$$\delta D = \frac{\mathrm{AD}-\mathrm{BC}}{2} = \frac{\Delta\eta}{\sin\theta} + \frac{\Delta\xi'}{\cos\theta},$$

$$\langle D\rangle = \frac{\mathrm{AD}+\mathrm{BC}}{2} = \frac{\langle\xi'\rangle-\langle\xi\rangle}{\cos\theta} = \frac{\langle\eta'\rangle-\langle\eta\rangle}{\sin\theta},$$

where the last equality is easily seen to follow from the geometry of Fig 12. Thus, for the case HV

$$\left(\frac{\delta D}{\langle D\rangle}\right)_{\mathrm{HV}} = \frac{\Delta\xi'}{\langle\xi'\rangle-\langle\xi\rangle} + \frac{\Delta\eta}{\langle\eta'\rangle-\langle\eta\rangle}. \tag{96}$$

We then find the relative error for case VH by interchanging η and ξ in equation (96):

$$\left(\frac{\delta D}{\langle D\rangle}\right)_{\mathrm{VH}} = \frac{\Delta\xi}{\langle\xi'\rangle-\langle\xi\rangle} + \frac{\Delta\eta'}{\langle\eta'\rangle-\langle\eta\rangle}. \tag{97}$$

Similarly, the relative error for case HH is obtained by making the same interchange in equation (95):

$$\left(\frac{\delta D}{\langle D\rangle}\right)_{\mathrm{HH}} = \frac{\Delta\eta+\Delta\eta'}{\langle\eta'\rangle-\langle\eta\rangle}. \tag{98}$$

As we mentioned before, the cases of α and β correspond to the following replacements in expressions (95,96,97,98) and conditions (91,92):

$$\alpha \; : \; (\xi,\eta) = (x,y)\,; \quad (\xi',\eta') = (x_0,y_0), \tag{99}$$

$$\beta \; : \; (\xi,\eta) = (x_0,y_0)\,; \; (\xi',\eta') = (x_1,y_1). \tag{100}$$

(Recall that for the uncertainty rectangle R of the FOE, $(\langle x\rangle,\langle y\rangle) = (0,0)$.) We then find the analytic expressions which determine whether the NDP passes through the H– or

V-side of the uncertainty rectangles R, R_0, and R_1. Noting that for all the uncertainty rectangles the slope of the NDP is, given our assumptions, just $m = \langle y_0 \rangle / \langle x_0 \rangle$, we find

- The NDP passes through the H (V) side of R if

$$\frac{\Delta y}{\Delta x} > (<) \frac{\langle y_0 \rangle}{\langle x_0 \rangle}. \tag{101}$$

- The NDP passes through the H (V) side of R_0 if

$$\frac{\Delta y_0}{\Delta x_0} > (<) \frac{\langle y_0 \rangle}{\langle x_0 \rangle}. \tag{102}$$

- The NDP passes through the H (V) side of R_1 if

$$\frac{\Delta y_1}{\Delta x_1} > (<) \frac{\langle y_0 \rangle}{\langle x_0 \rangle}. \tag{103}$$

Using the appropriate replacements (99,100) in expressions (95,96,97,98), we find the expressions for the relative uncertainties α and β:

Case VV

$$\begin{aligned} \alpha &= \frac{\Delta x}{\langle x_0 \rangle} + \frac{\Delta x_0}{\langle x_0 \rangle}; \\ \beta &= \frac{\Delta x_1 + \Delta x_0}{\langle x_1 \rangle - \langle x_0 \rangle} = \left[\frac{1}{\langle K_0 \rangle - 1}\right] \cdot \left[\frac{\Delta x_0}{\langle x_0 \rangle} + \frac{\Delta x_1}{\langle x_0 \rangle}\right]. \end{aligned} \tag{104}$$

Case HV

$$\begin{aligned} \alpha &= \frac{\Delta x_0}{\langle x_0 \rangle} + \frac{\Delta y}{\langle y_0 \rangle}; \\ \beta &= \frac{\Delta x_1}{\langle x_1 \rangle - \langle x_0 \rangle} + \frac{\Delta y_0}{\langle y_1 \rangle - \langle y_0 \rangle} = \left[\frac{1}{\langle K_0 \rangle - 1}\right] \cdot \left[\frac{\Delta x_1}{\langle x_0 \rangle} + \frac{\Delta y_0}{\langle y_0 \rangle}\right]. \end{aligned} \tag{105}$$

Case VH

$$\alpha = \frac{\Delta x}{\langle x_0 \rangle} + \frac{\Delta y_0}{\langle y_0 \rangle};$$

$$\beta = \frac{\Delta x_0}{\langle x_1 \rangle - \langle x_0 \rangle} + \frac{\Delta y_1}{\langle y_1 \rangle - \langle y_0 \rangle} = \left[\frac{1}{\langle K_0 \rangle - 1}\right] \cdot \left[\frac{\Delta x_0}{\langle x_0 \rangle} + \frac{\Delta y_1}{\langle y_0 \rangle}\right]. \tag{106}$$

Case HH

$$\alpha = \frac{\Delta y}{\langle y_0 \rangle} + \frac{\Delta y_0}{\langle y_0 \rangle};$$

$$\beta = \frac{\Delta y_1 + \Delta y_0}{\langle y_1 \rangle - \langle y_0 \rangle} = \left[\frac{1}{\langle K_0 \rangle - 1}\right] \cdot \left[\frac{\Delta y_0}{\langle y_0 \rangle} + \frac{\Delta y_1}{\langle y_0 \rangle}\right]. \tag{107}$$

We have used equation (9) to express β in terms of $\langle K_0 \rangle$. Note that the expressions for α and β in case VH (HH) are obtained from those in the case HV (VV) by interchanging x and y, as expected.

In order that the list above not be misunderstood, note that the listing of the expression for α together with that for β under each of the four possible cases is for economy only; the "case" description for α refers to a different pair of uncertainty rectangles than for β, i.e., "case VV" refers to how the NDP passes through R and R_0 (for α), and how it passes through R_0 and R_1 (for β).

The relative uncertainties α and β are calculated from the three uncertainty rectangles R, R_0, and R_1, and depend on how the NDP passes through these uncertainty rectangles. We use the symbol ijk, where each of i, j, and k can be either H or V, to denote the side of R, R_0, and R_1, respectively, through which the NDP passes. Thus, the case HVH is that for which the NDP passes through the horizontal (H) side of R, the vertical (V) side of R_0, and the horizontal (H) side of R_1. There are thus eight possible cases to consider[4]: VVV, VHV, VVH, VHH, HVV, HHV, HVH, and HHH. We can obtain the appropriate expressions for any one of these cases as follows. For the case ijk, α is given by the expression in case ij of equations (104)...(107), and β by the expression in case jk of equations (104)...(107). For instance, in the case VHV (see Figure 15) we have

$$\alpha = \frac{\Delta x}{\langle x_0 \rangle} + \frac{\Delta y_0}{\langle y_0 \rangle}, \tag{108}$$

as is given in case VH (equation (106)), and

$$\beta = \left[\frac{1}{\langle K_0 \rangle - 1}\right] \cdot \left[\frac{\Delta x_1}{\langle x_0 \rangle} + \frac{\Delta y_0}{\langle y_0 \rangle}\right], \tag{109}$$

as is given in case HV (equation(105)). The other seven cases are found in an identical fashion. Note that there are really only four independent cases, since interchanging H and V in the case ijk is equivalent to interchanging x and y in the corresponding expressions for α and β.

D Summary of the numerical results

We summarize here the results of our calculations for the search regions. All rectangles have center at (C_x, C_y) (see (33)) and sides $\{2S_x, S_y\}$ (see (34)).

D.1 The search region $\mathcal{R}_1$

The phrase "overlap on the ω-axis" means that the projections of R and R_0 onto the ω-axis overlap, i.e., that $\langle \omega_0 \rangle < \Delta\omega + \Delta\omega_0$.

[4] We again note that if the NDP passes through the corners of a particular uncertainty rectangle, the corner can be considered either an H-side or a V-side; the same results are obtained for either choice.

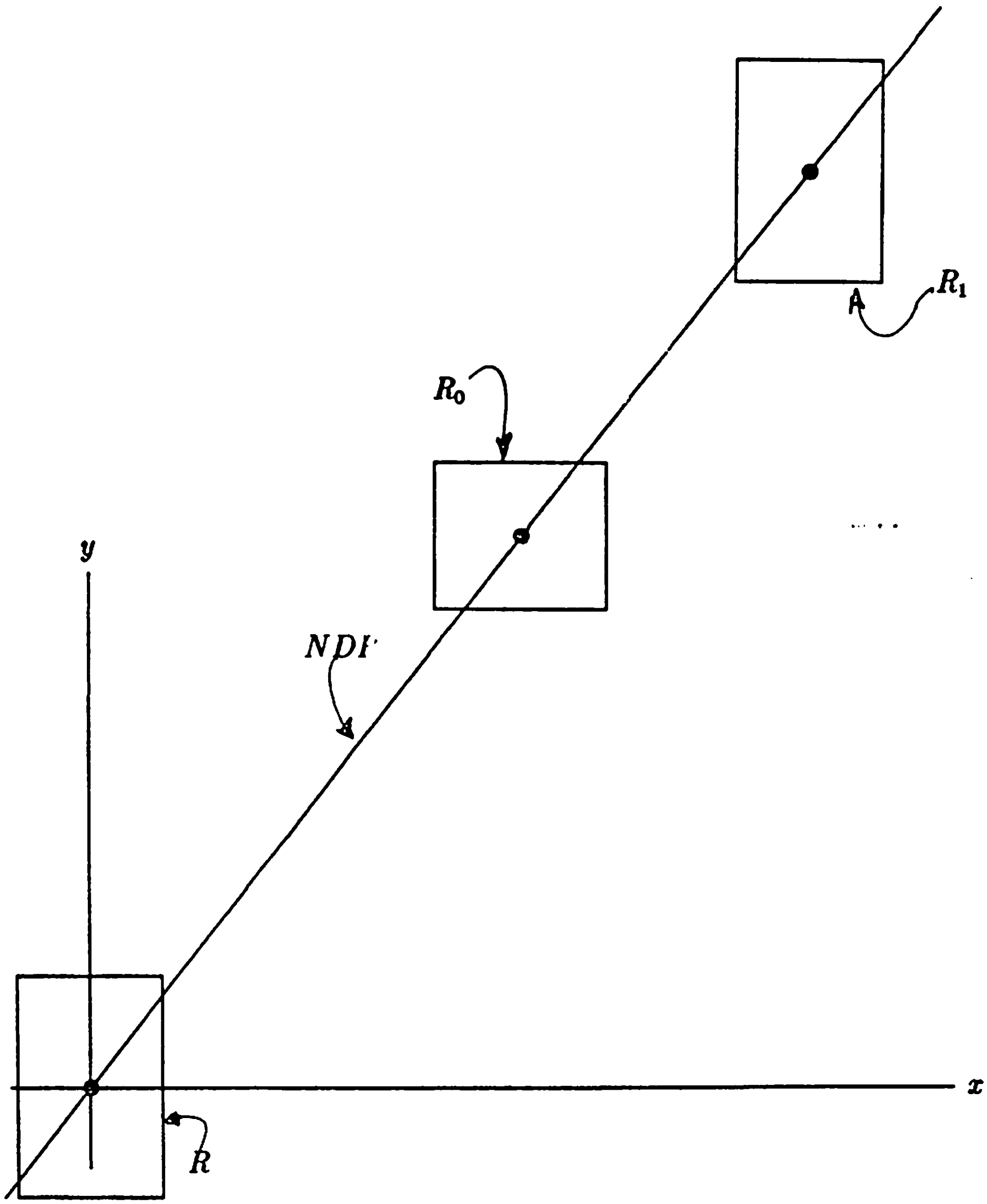

Figure 15: **Case VHV**: the NDP passes through the vertical sides of R and R_1, and the horizontal sides of R_0.

I. Search region $\mathcal{R}_1$ for accurate Z_0 and T

$$
\begin{aligned}
C_x &= K_0\langle x_0\rangle \\
C_y &= K_0\langle y_0\rangle \\
S_x &= K_0\Delta x_0 + (K_0 - 1)\Delta x \\
S_y &= K_0\Delta y_0 + (K_0 - 1)\Delta y.
\end{aligned}
$$

II. Search region $\mathcal{R}_1$ for uncertain Z_0 and T

In these cases, the search region $\mathcal{R}_1$ is the intersection of a wedge and the rectangle R_1^*. The quantity ϵ is given by equation (28):

$$\epsilon = \frac{\delta Z_0}{\langle Z_0\rangle} + \frac{\delta T}{\langle T\rangle}.$$

II.1 Non–overlapping case

In this case we have $\langle x_0\rangle > \Delta x + \Delta x_0$, $\langle y_0\rangle > \Delta y + \Delta y_0$ (see Figure 16).

WEDGE

$$y_{\min}(x) \le y \le y_{\max}, \tag{110}$$

where

$$y_{\min}^{\max}(x) = (x \mp \Delta x)\left[\frac{\langle y_0\rangle \pm (\Delta y + \Delta y_0)}{\langle x_0\rangle \mp (\Delta x + \Delta x_0)}\right] \mp \Delta y \ . \tag{111}$$

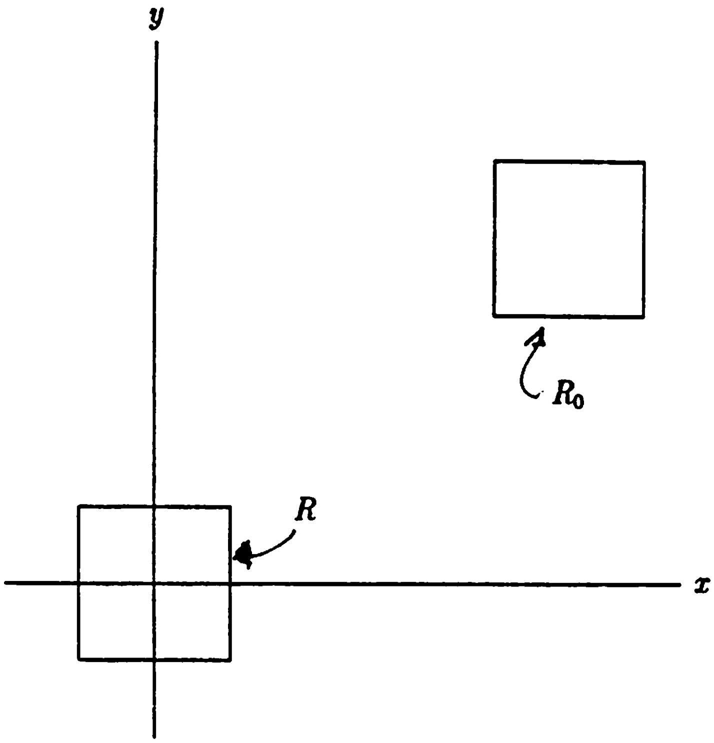

Figure 16: The "non–overlapping" case II.1. Neither of the projections of the rectangles onto the coördinate axes overlap.

RECTANGLE

$$C_x = \langle K_0\rangle\langle x_0\rangle\left\{1+(\langle K_0\rangle-1)\,[\epsilon]\left[\frac{\Delta x+\Delta x_0}{\langle x_0\rangle}\right]\right\}$$

$$C_y = \langle K_0\rangle\langle y_0\rangle\left\{1+(\langle K_0\rangle-1)\,[\epsilon]\left[\frac{\Delta y+\Delta y_0}{\langle y_0\rangle}\right]\right\}$$

$$S_x = \langle K_0\rangle\Delta x_0+(\langle K_0\rangle-1)\Delta x+\langle K_0\rangle(\langle K_0\rangle-1)[\epsilon]\,\{\langle x_0\rangle\}$$

$$S_y = \langle K_0\rangle\Delta y_0+(\langle K_0\rangle-1)\Delta y+\langle K_0\rangle(\langle K_0\rangle-1)[\epsilon]\,\{\langle y_0\rangle\}\,.$$

II.2 Overlapping on the y–axis, but not on the x–axis

In this case we have $\langle x_0\rangle > \Delta x+\Delta x_0$, $\langle y_0\rangle < \Delta y+\Delta y_0$ (see Figure 17).

WEDGE

$$y_{\min}(x) \le y \le y_{\max}, \tag{112}$$

where

$$y^{\max}_{\min}(x) = (x - \Delta x)\left[\frac{\langle y_0\rangle \mp (\Delta y + \Delta y_0)}{\langle x_0\rangle - (\Delta x + \Delta x_0)}\right] \pm \Delta y\ . \tag{113}$$

RECTANGLE

$$\begin{aligned}
C_x &= \langle K_0\rangle\langle x_0\rangle \left\{1 + (\langle K_0\rangle - 1)\,[\epsilon]\left[\frac{\Delta x + \Delta x_0}{\langle x_0\rangle}\right]\right\} \\
C_y &= \langle K_0\rangle\langle y_0\rangle \left\{1 + (\langle K_0\rangle - 1)\,[\epsilon]\right\} \\
S_x &= \langle K_0\rangle\Delta x_0 + (\langle K_0\rangle - 1)\Delta x + \langle K_0\rangle(\langle K_0\rangle - 1)[\epsilon]\,\{\langle x_0\rangle\} \\
S_y &= \langle K_0\rangle\Delta y_0 + (\langle K_0\rangle - 1)\Delta y + \langle K_0\rangle(\langle K_0\rangle - 1)[\epsilon]\,\{\Delta y + \Delta y_0\}\,.
\end{aligned}$$

II.3 Overlapping on the x–axis, but not on the y–axis

In this case we have $\langle x_0\rangle < \Delta x + \Delta x_0$, $\langle y_0\rangle > \Delta y + \Delta y_0$ (see Figure 18).

WEDGE

$$x_{\min}(y) \le x \le x_{\max}, \tag{114}$$

where

$$x^{\max}_{\min}(y) = (y - \Delta y)\left[\frac{\langle x_0\rangle \mp (\Delta x + \Delta x_0)}{\langle y_0\rangle - (\Delta y + \Delta y_0)}\right] \pm \Delta x. \tag{115}$$

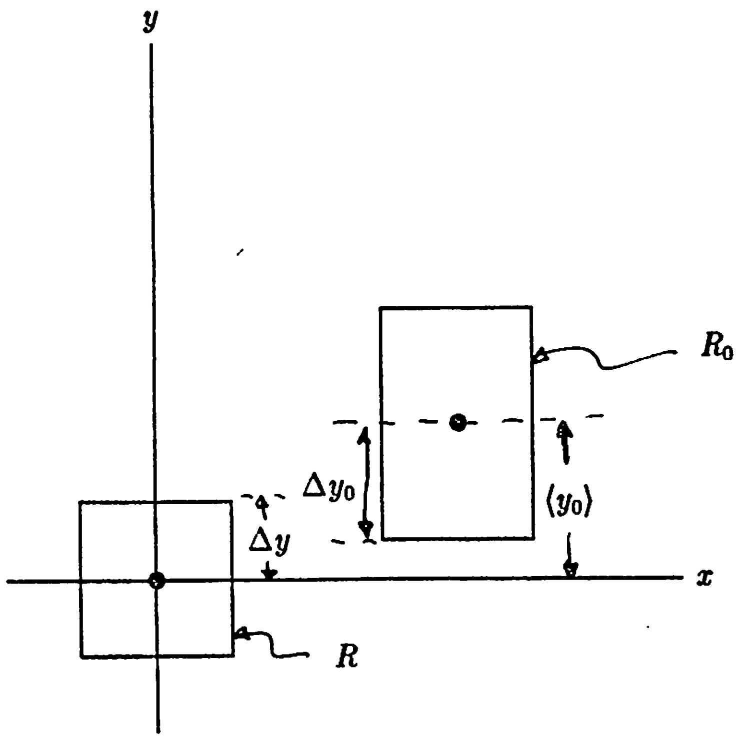

Figure 17: Case II.2. The projections of the rectangles R and R_0 overlap on the y–axis

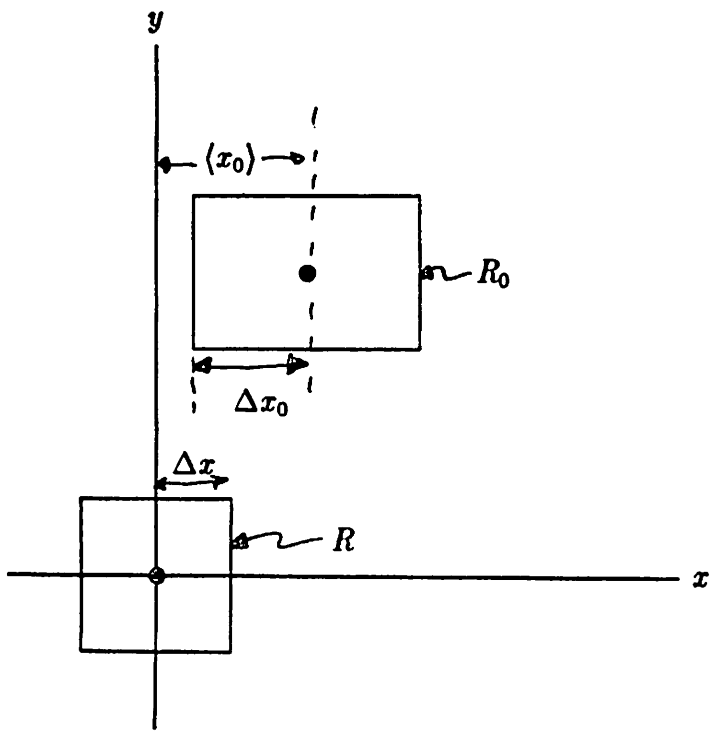

Figure 18: Case II.3. The projections of the rectangles R and R_0 overlap on the x–axis

RECTANGLE

$$
\begin{aligned}
C_x &= \langle K_0\rangle\langle x_0\rangle \{1 + (\langle K_0\rangle - 1)\,[\epsilon]\} \\
C_y &= \langle K_0\rangle\langle y_0\rangle \left\{1 + (\langle K_0\rangle - 1)\,[\epsilon]\left[\frac{\Delta y + \Delta y_0}{\langle y_0\rangle}\right]\right\} \\
S_x &= \langle K_0\rangle\Delta x_0 + (\langle K_0\rangle - 1)\Delta x + \langle K_0\rangle(\langle K_0\rangle - 1)[\epsilon]\,\{\Delta x + \Delta x_0\} \\
S_y &= \langle K_0\rangle\Delta y_0 + (\langle K_0\rangle - 1)\Delta y + \langle K_0\rangle(\langle K_0\rangle - 1)[\epsilon]\,\{\langle y_0\rangle\}\,.
\end{aligned}
$$

D.2 The search region $\mathcal{R}_2$

We summarize here the results for the search region $\mathcal{R}_2$ for the image point F_2 in the third frame. As noted in Section 4.3, these results are obtained from those for $\mathcal{R}_1$ by making certain replacements. The replacements are

- Replace $\langle K_0 \rangle$ by $K_1^{\rm mean}$ and $\langle Z_0 \rangle$ by $Z_1^{\rm mean}$.

- Replace all "0" subscripts by "1" subscripts.

Doing so, we find the following results. In each case, $Z_1^{\rm mean}$ and δZ_1 are given by (44) and (45), respectively, and

$$K_1^{\rm mean} = \frac{Z_1^{\rm mean}}{Z_1^{\rm mean} - \langle T \rangle} \ . \tag{116}$$

The quantity ϵ is now just equal to $\delta Z_1 / Z_1^{\rm mean}$, since we assumed accurately known T.

III. Search region $\mathcal{R}_2$ for uncertain FOE, F_0, and F_1.

In these cases, the search region $\mathcal{R}_2$ is the intersection of a wedge and the rectangle R_2^*. "Overlap" now refers to R and R_1.

III.1 Non–overlapping case

In this case we have $\langle x_1 \rangle > \Delta x + \Delta x_1$, $\langle y_1 \rangle > \Delta y + \Delta y_1$.

WEDGE

$$y_{\rm min}(x) \leq y \leq y_{\rm max}, \tag{117}$$

where

$$y_{\rm min}^{\rm max}(x) = (x \mp \Delta x) \left[\frac{\langle y_1 \rangle \pm (\Delta y + \Delta y_1)}{\langle x_1 \rangle \mp (\Delta x + \Delta x_1)} \right] \mp \Delta y \ . \tag{118}$$

RECTANGLE

$$
\begin{aligned}
C_x &= K_1^{\rm mean}\langle x_1\rangle \left\{1 + (K_1^{\rm mean} - 1)\,[\epsilon]\left[\frac{\Delta x + \Delta x_1}{\langle x_1\rangle}\right]\right\} \\
C_y &= K_1^{\rm mean}\langle y_1\rangle \left\{1 + (K_1^{\rm mean} - 1)\,[\epsilon]\left[\frac{\Delta y + \Delta y_1}{\langle y_1\rangle}\right]\right\} \\
S_x &= K_1^{\rm mean}\Delta x_1 + (K_1^{\rm mean} - 1)\Delta x + K_1^{\rm mean}(K_1^{\rm mean} - 1)[\epsilon]\,\{\langle x_1\rangle\} \\
S_y &= K_1^{\rm mean}\Delta y_1 + (K_1^{\rm mean} - 1)\Delta y + K_1^{\rm mean}(K_1^{\rm mean} - 1)[\epsilon]\,\{\langle y_1\rangle\}\,.
\end{aligned}
$$

III.2 Overlapping on the y–axis, but not on the x–axis

In this case we have $\langle x_1\rangle > \Delta x + \Delta x_1$, $\langle y_1\rangle < \Delta y + \Delta y_1$ (see Figure 17).

WEDGE

$$y_{\rm min}(x) \le y \le y_{\rm max}, \tag{119}$$

where

$$y_{\rm min}^{\rm max}(x) = (x - \Delta x)\left[\frac{\langle y_1\rangle \mp (\Delta y + \Delta y_1)}{\langle x_1\rangle - (\Delta x + \Delta x_1)}\right] \pm \Delta y\,. \tag{120}$$

RECTANGLE

$$
\begin{aligned}
C_x &= K_1^{\rm mean}\langle x_1\rangle \left\{1 + (K_1^{\rm mean} - 1)\,[\epsilon]\left[\frac{\Delta x + \Delta x_1}{\langle x_1\rangle}\right]\right\} \\
C_y &= K_1^{\rm mean}\langle y_1\rangle \,\{1 + (K_1^{\rm mean} - 1)\,[\epsilon]\} \\
S_x &= K_1^{\rm mean}\Delta x_1 + (K_1^{\rm mean} - 1)\Delta x + K_1^{\rm mean}(K_1^{\rm mean} - 1)[\epsilon]\,\{\langle x_1\rangle\} \\
S_y &= K_1^{\rm mean}\Delta y_1 + (K_1^{\rm mean} - 1)\Delta y + K_1^{\rm mean}(K_1^{\rm mean} - 1)[\epsilon]\,\{\Delta y + \Delta y_1\}\,.
\end{aligned}
$$

III.3 Overlapping on the x–axis, but not on the y–axis

In this case we have $\langle x_1 \rangle < \Delta x + \Delta x_1$, $\langle y_1 \rangle > \Delta y + \Delta y_1$ (see Figure 18).

WEDGE

$$x_{\min}(y) \leq x \leq x_{\max}(y), \tag{121}$$

where

$$x_{\min}^{\max}(y) = (y - \Delta y)\left[\frac{\langle x_1 \rangle \mp (\Delta x + \Delta x_1)}{\langle y_1 \rangle - (\Delta y + \Delta y_1)}\right] \pm \Delta x. \tag{122}$$

RECTANGLE

$$\begin{aligned}
C_x &= K_1^{\text{mean}} \langle x_1 \rangle \left\{1 + (K_1^{\text{mean}} - 1)\,[\epsilon]\right\} \\
C_y &= K_1^{\text{mean}} \langle y_1 \rangle \left\{1 + (K_1^{\text{mean}} - 1)\,[\epsilon]\left[\frac{\Delta y + \Delta y_1}{\langle y_1 \rangle}\right]\right\} \\
S_x &= K_1^{\text{mean}} \Delta x_1 + (K_1^{\text{mean}} - 1)\Delta x + K_1^{\text{mean}}(K_1^{\text{mean}} - 1)[\epsilon]\left\{\Delta x + \Delta x_1\right\} \\
S_y &= K_1^{\text{mean}} \Delta y_1 + (K_1^{\text{mean}} - 1)\Delta y + K_1^{\text{mean}}(K_1^{\text{mean}} - 1)[\epsilon]\left\{\langle y_1 \rangle\right\}.
\end{aligned}$$